Geol. Paläont. Mitt. Innsbruck, ISSN 0378–6870, Band 26, S. 109–136, 2003

LOCAL AND FAR FIELD STRESS-ANALYSIS OF BRITTLE DEFORMATION IN THE WESTERN PART OF THE NORTHERN CALCAREOUS ALPS, AUSTRIA

Hugo Ortner

With 25 figures and 1 table

Abstract

Brittle deformation was analysed in 86 stations with in the western Northern Calcareous Alps (NCA). Six paleostress tensor groups were defined, which constrain the deformational history since onset of Alpine deformation and can be related to distinct stages of deformation in other parts of the orogen. The superposition of deformational events with stress tensors of the same geometry, but different ages was estblished. The evolution of the far field stresses (1st order stress), which are thought to be related to plate movements, was simple: Cretaceous NW-directed compression was followed by Paleocene/Eocene NNE-directed compression, which in turn was replaced by Oligocene/Miocene NNW-directed compression. Local stress fields (2nd order stress) complicate the picture: Cretaceous NW-compression was partitioned into NNW-directed compression in the NCA and W-directed compression in the Central Alps. Oligocene/Miocene NNW-directed compression was superposed by secondary stress fields related to lateral escape of crustal blocks during formation of the metamorphic core complex of the Tauern Window: N- to NNE-directed compression near large faults delimiting eastward moving blocks and E-directed extension. Third order stress fields are related to folding. The succession of these 3rd order stress fields is not systematic. Additionally, stress tensors related to Late Miocene E-W compression were recorded, which are related to collision in the Carpathian orogen.

1 Introduction

The study of brittle deformation in polyphasely deformed orogens has three fundamental difficulties: (i) the problem to separate inhomogeneous fault data sets into homogeneous subsets without previous knowledge of the shape of the involved stress tensors; (ii) the ages of paleostress tensors are usually poorly defined, in most cases only relative ages between individual deformational events can be defined; (iii) the interpretation of the deduced stress tensors either being equivalent to far-field stress parallel to the plate movement vector or representing local stress fields created inside or near large shear zones. Timing of deformations can be established when investigating deformation in successively younger syntectonic sediments (e.g. Kleinspehn et al., 1989) and soft-sediment deformation, occuring prior to complete lithification of the rocks (e.g. Petit & Laville, 1987). Comparing brittle deformation in different parts of the orogen, e.g. in the internal and external part or in the foreland- and the hinterland directed wedge can help to distinguish between local and far-field stresses, because the different parts of the orogen may be affected by different processes, and the associated stress fields should only be recorded in the respective part of the orogen.

This paper presents the results of an extensive field study on soft-sediment and brittle deformation in the northwestern part of the Eastern Alps. The results are compared to published data on brittle deformation of the Southern and Eastern Alps, and some principles for interpretation of results of regional studies of brittle deformation are deduced.

1.1 Geological setting

1.1.1 Deformation within the Northern Calcareous Alps (NCA)

The thrust sheets of the NCA are the highest tectonic units of the Austroalpine nappe complex. Deformation related to Alpine orogeny started in the early Late Cretaceous, when the principal thrust architecture of the NCA was established by (N)NW-directed thrusting (Eisbacher & Brandner, 1996; Ortner, 2001) in the foreland of the closure of the Meliata ocean (Froitzheim et al. 1994, 1996; Neubauer et al., 2000). Continental collision between the (upper) Adriatic microplate and the European (lower) plate related to closure of the Penninic

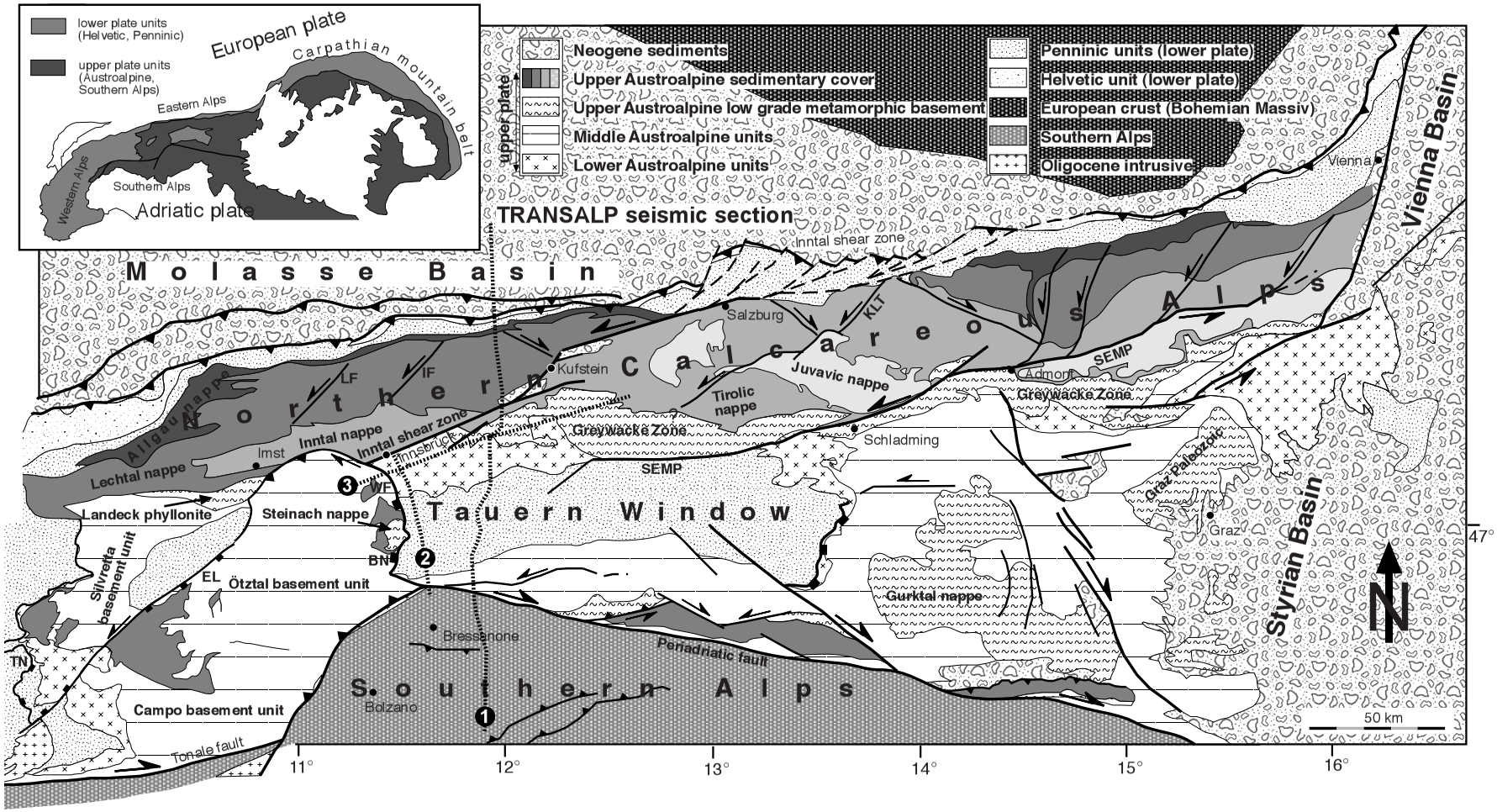

Fig. 1: Simplified geological overview of the Eastern Alps. Thick black lines delineate young (Oligocene and Miocene) faults. TN = Turba normal fault, EL = Engadine line, LF = Loisach fault, IF = Isartal fault, BN = Brenner normal fault, WP = Wipptal fault, SEMP = Salzachtal-Ennstal-Mariazell-Puchberg line, KLT = Königssee-Lammertal-Traunsee line. Numbers 1 – 4 indicate positions of cross sections.

oceans and subsequent post-collisional shortening was responsible for Eocene to Miocene deformation within the NCA and accreted units of the Penninic ocean (Flysch units), of the distal European margin (Helvetic units) and the allochthonous Molasse. In the more internal parts of the Alpine chain, Oligocene and Miocene out-of-sequence thrusting and backthrusting led to exhumation of the Tauern Window accompanied by major orogen-parallel extension (Lammerer & Weger, 1998), combined with a generally E-directed flow of material. According to Ratschbacher et al. (1991), the eastward moving blocks were delimited to the north by major ENE-striking faults: from E to W these are the SEMP-line and several faults branching from it, the KLT-line and the Inntal shear zone, that cut the NCA obliquely (Fig. 1). Oblique backthrusting along the Periadriatic line at the southern margin of the Eastern Alps propagated into the footwall and towards the south, leading to south-directed thrusting in the southern Alps until recent times, whereas orogen-parallel extension in the Eastern Alps came to an end in the Late Miocene (Peresson & Decker, 1997).

The TRANSALP seismic section (Fig. 2) shed new light on the 3D geometry of the Alps and the Inntal shear zone, revealing a major south-dipping thrust reaching the surface at the southern margin of the Inn Valley, which superimposes metamorphic Paleozoic units onto the Northern Calcareous Alps with a throw of approximately 10km (Fig. 2; TRANSALP Working Group, 2001). At the surface, the Inntal shear zone appears to be a major subvertical ENE-trending strike-slip fault. Much has been speculated about the sinistral offset of the Inntal fault, with estimates ranging from 75 km (Frisch et al., 1998) to about 40 km (Ortner et al., 1999). Taking into account the possible thrust fault geometry of the Inntal shear zone, part of the apparent sinistral offset in map view might be produced by thrusting.

1.1.2 Synorogenic sediments

Late Eocene (Priabonian) deposits represent the oldest part of the Alpine Molasse basin on top of the NCA with terrestrial to shallow marine deposits (Oberaudorf beds). After a short period of erosion and/or non-deposition, Oligocene sedimentation started with limnofluviatile deposits (Häring Fm.). The depositional realm rapidly subsided to pelagic conditions (Paisslberg Fm.). In the Late Rupelian, a

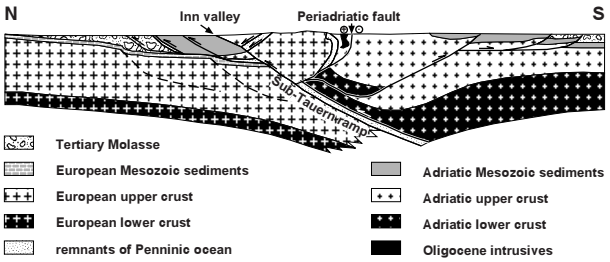

Fig. 2: Interpretation of the TRANSALP deep seismic section redrawn from TRANSALP Working Group (2002), according to their "lateral extrusion model". Length of section = 300 km.

delta started to prograde from the west (Unterangerberg Fm.). Fluviatile sedimentation resumed in the Late Oligocene (Oberangerberg Fm.). Because of the many similarities with deposits in the Molasse basin, the Oligocene of the Lower Inn Valley was also termed „Inneralpine Molasse" (Fuchs, 1976, 1980; Ortner & Stingl, 2001). A detailed description of the sedimentary succession is found in Ortner & Stingl (2001).

2 Deformational structures observed

2.1 Synsedimentary deformation in the Oligocene intra-Alpine Molasse deposits

The depositional geometries of Lower Oligocene sediments were strongly influenced by synsedimentary shearing (for a more detailed description, see Ortner & Stingl, 2001). Bituminous marls of the Häring Fm. were deposited in decametric half grabens along faults (Fig. 3a). Deposits of cobbles and boulders at the basin margins associated with sediment infilling and draping with bituminous marls are interpreted as scarp breccias. Towards the footwall, the breccias pass into intact rock without sharp boundary. In some meters distance toward the basin, isolated blocks of up to 1/2 m size are found within the bituminous marls, derived from the footwall of the basin margin fault. Neptunian dykes filled with debris of Oligocene carbonates of the Werlberg Mb. all trend NW-SE (Fig. 3c). Locally, slickensides are preserved on the walls of these dykes, which indicate a dextral normal sense of shear (Fig. 3b, faults with grey symbols). Therefore dextral shearing along WNW trending faults was active during deposition of the Häring and Paisslberg Fms.

With an increase in sand-sized detritus shed into the basin, the Unterangerberg Fm. develops from

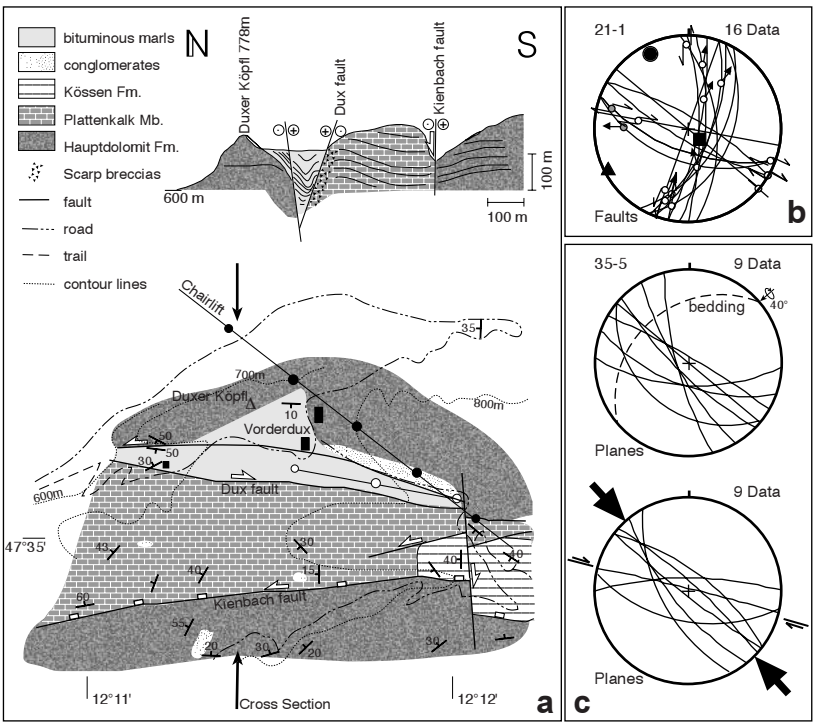

Fig. 3: a) Geological sketch and cross section of the Dux syncline S of Kufstein, illustrating the half graben geometry of Rupelian basins. b) Faults from the Grattenberg locality. Two faults are sealed by neptunian dykes (grey symbols). c) orientations of neptunian dykes filled with Oligocene sediments. Top: uncorrected orientations. bottom: orientations after backtilting of bedding of overlying bituminous marls to horizontal. A possible interpretation as shear and tension joints is indicated.

the Paisslberg Fm. The Unterangerberg Fm. is dominated by turbiditic sand/mud couplets. Deformation of these sediments started during deposition and accompanied and outlasted diagenesis. Accordingly, deformational structures change depending on the decreasing viscosity of the lithifying sediments and the increasing strain superimposed on the sediments.

The oldest deformational structures are slump folds at the base of sandstone beds. Fold axes of slump folds are consistently orthogonal to flute and groove casts, which are NW-SE-trending. Commonly the size of slump folds is approximately on the dimension of bed thickness. In contrast, structures of soft sediment deformation are usually only a fraction of bed thickness in size. In the hangingwall of a shear zone, deformational structures illustrate increasing bedding-parallel shortening: Cuspate-lobate structures are found at the sharp lower interface between sandstone and marl beds, but not on the gradational upper interface (Fig 3c, d; Fig. 14b of Ortner & Stingl, 2003, this volume). At locations with more lithified sandstone beds, shortening is taken up by blind thrusts, but the horizontal top of the bed is preserved (Fig. 14d of Ortner & Stingl, 2003, this volume). Hydroplastic slickensides (Petit & Laville, 1987), indicating shearing in partly lithified sediment, are found on small ramps in sandstone beds, leading to stacking of sandstone beds (Fig 3a, b; Fig. 14d of Ortner & Stingl, 2003, this volume). The shear zone itself is characterized by an interval several meters thick, where bedding is overprinted by a foliation and sandstone beds are disrupted and the fragments isoclinally folded (Fig. 14f of Ortner & Stingl, 2003, this volume). The long axes of the cuspate-lobate structures and intersection lineations of ramps with bedding trend NW-SE (Fig. 3c-d), movement in the shear zone is top to SW. Deformation continued after lithification and led to decametric folding above the shear zone with still NW-trending fold axes. Locally, also E-W striking vertical shear zones with sandstone beds isoclinally folded around vertical axes arefound.

As demonstrated above, a major change in the geometry of the stress field took place during the Rupelian or near the boundary from Rupelian to Chattian. Before and during the Rupelian, NNW-SSE contraction was active, followed by NNE-SSW contraction from the latest Rupelian or Chattian onwards.

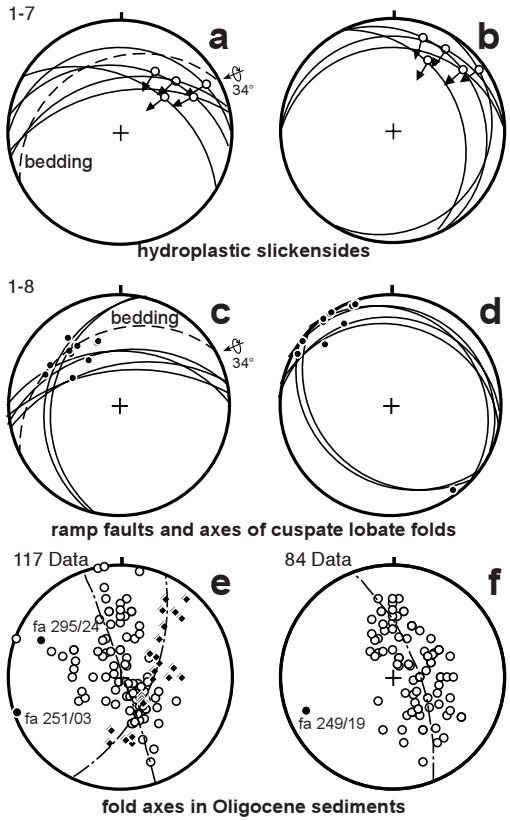

Fig. 4: Structural data from the Angerberg area: a) Orientation of hydroplastic slickensides in Unterangerberg Fm. b) Orientation of hydroplastic slickensides after rotation of bedding to horizontal. c) Orientation of long axes of cuspate lobate folds (black symbols) and ramps (great circles) in Unterangerberg Fm. d) Orientation of long axes of cuspate lobate folds (black symbols) and ramps (great circles) after rotation of bedding to horizontal. e) Orientation of bedding planes Unterangerberg Fm. Black diamonds indicate bedding in folds considered to be related to Early Rupelian folding. f) Orientation of bedding planes Oberangerberg Fm.

2.2 Postsedimentary brittle deformation

2.2.1 Methods

In the field, brittle faults (Petit, 1987), tension gashes, joints and stylolithes (Hancock, 1985) were measured in sediments of known age. Geometrically inhomogeneous datasets were split into homogeneous subsets taking into account crosscutting and overprinting relationships. Datasets with fault geometries indicative of non-coaxial deformation were interpreted to represent increments of shearing (Woijtal & Pershing, 1991). Noncoaxial shearing can be recognized, when a prinicipal displacement zone and conjugate Riedel and Antiriedel shears are present, which are usually more abundant, because they develop prior to the throughgoing larger shear zone (Mandl, 1988), which only connects older synthetic Riedel shears. A kinematic interpretation was done to determine the orientation of compression and extension to be able to compare non-coaxial datasets with coaxial datasets. For doing this, the orientation of the kinematical axes was calculated with the NDA method (Sperner et al., 1993), and checked whether the compressional axis was located half way between Riedel and Antiriedel shears, as these represent the local stress field within the shear zone. For coaxial datasets, the orientation of kinematical axes was calculated with the NDA method, using an angle of 30° between slip line and the compressional axis. The kinematical axes are considered to coincide with the principal stress axes σ_1, σ_2 and σ_3 ($\sigma_1>\sigma_2>\sigma_3$). The direct inversion method (Angelier & Goguel, 1979) proved to be unreliable if fault planes were not distributed evenly in space, which was the case in many fault data sets. The analysis of all tectonic data was done with the software TectonicVB (Ortner et al., 2002). The results are presented in Table 1.

Fault data were recorded inside and outside of major shear zones to evaluate the role of shear zones during distinct deformational events. Fault data sets were grouped according to the orientations of their principal stress axes. The succession of

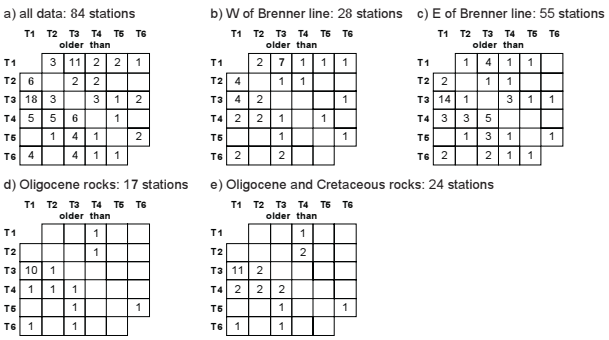

Fig. 5: Discrimination matrices of different subsets of data. a) All data. Cross cutting relationships are not systematic. b) All data west of Brenner normal fault. Most of the data indicating T3 (NNE-SSW-contraction) older than T1 (NNW-SSE contraction) come from outcrops near the Engadine line. There, T1 is possibly related to the Domleschg phase of Froitzheim et al., 1994). c) all data east of the Brenner normal fault. Cross cutting relationships indicating T3 older T1 are from localities, where Oligocene or Cretaceous NNE-contraction predates Miocene NNW-contraction. d) data from Oligocene rocks. e) data from Oligocene and Cretaceous rocks. c) and d) show, that the relative ages are not defined for all events.

No.	Location	Age of rock	X_{6KM} BMN	Y_M BMN	Method	N	σ_1	σ_2	σ_3	Geometry	Group
1	Oberangerberg	Chattian/Oligocene	345000	261000	NDA	9	337 / 6	220 / 75	68 / 12	pure shear	T1
					NDA	14	190 / 5	281 / 11	75 / 77	pure shear	T2
2	Schindler	Rupelian/Oligocene	344600	261550	NDA	6	7 / 6	98 / 9	243 / 78	pure shear	T2
3	Silz: W Steinbruch	Anisian/Early Triassic	194550	237325	kinematic interpretation	14	229 / 0	126 / 69	319 / 19	simple shear	T3
					NDA	10	31 / 85	251 / 3	161 / 3	pure shear	T6
					NDA	5	316 / 61	157 / 26	63 / 8	pure shear	T4
5	Zirl: Schloßbachklamm	Ladinian/Triassic	218625	238325	kinematic interpretation	13	339 / 2	241 / 70	70 / 19	simple shear	T1
					NDA	7	184 / 83	324 / 4	54 / 4	pure shear	T4
6	Zirl: Ehnbachklamm	Carnian/Triassic	219475	237750	NDA	5	135 / 0	234 / 83	45 / 6	pure shear	T1
					NDA	6	342 / 11	250 / 10	117 / 74	pure shear	T1
					NDA	10	14 / 83	244 / 4	153 / 5	pure shear	T6
7	Zirl: Weinhof	Ladinian/Triassic	220125	237525	NDA	13	175 / 18	83 / 6	334 / 70	pure shear	T1
					NDA	6	154 / 15	307 / 72	62 / 7	pure shear	T1
					NDA	7	19 / 2	127 / 82	288 / 5	pure shear	T3
8	Kalkkögel: Kleiner Burgstall	Ladinian/Triassic	222887	222181	NDA	18	122 / 65	309 / 24	218 / 2	pure shear	T4
					Tension gashes	13			248 / 6	pure shear	T4
9	Kalkkögel: Halsl creek S of Axamer Lizum	Ladinian/Triassic	224245	228092	kinematic interpretation	33	181 / 8	20 / 80	272 / 2	simple shear	T2
					Right Dihedra	7	105 / 70	14 / 1	284 / 19	pure shear	T4
10	western side of Halltal (930m)	Ladinian/Triassic	239175	243014	NDA	9	30 / 20	202 / 68	299 / 2	pure shear	T3
					NDA	5	239 / 75	83 / 13	352 / 5	pure shear	T6
11	eastern side of Halltal (860m)	Ladinian/Triassic	239552	242598	kinematic interpretation	14	175 / 3	283 / 78	84 / 10	simple shear	T2
12	Vomper Berg: N of the Gasthof Bergblick	Norian/Triassic	248660	245392	kinematic interpretation	6	191 / 3	83 / 79	282 / 9	simple shear	T3
13	Vomper Loch gorge	Norian/Triassic	249552	245631	kinematic interpretation	17	180 / 11	81 / 37	284 / 50	simple shear	T3
14	Vomp: gravel pit Derfeser	postglacial/Quaternary	250207	244861	NDA	6	40 / 45	227 / 14	137 / 1	pure shear	T6
15	Schlitterberg	Devonian	261525	251175	kinematic interpretation	6	162 / 45	44 / 25	395 / 33	simple shear	T3
16	Oberangerberg: N of Mosen	Norian/Triassic	342325	259900	kinematic interpretation	11	9 / 5	114 / 70	277 / 18	simple shear	T3
			342325	259900	NDA	5	176 / 78	61 / 4	330 / 10	pure shear	T6
17	Oberangerberg: N of Berglsteiner See	Norian/Triassic	343000	260500	NDA	8	258 / 75	262 / 1	172 / 14	pure shear	T6
18	Bärengrube: N of Oberangerberg	Norian/Triassic	344125	261300	NDA	6	344 / 12	131 / 75	253 / 7	pure shear	T1
19	Kundler Klamm	Ladinian/Triassic	348725	258800	kinematic interpretation	21	20 / 6	131 / 73	288 / 15	simple shear	T3
			348725	258800	NDA	16	334 / 70	159 / 19	68 / 1	pure shear	T4
			348725	258800	NDA	8	107 / 42	301 / 46	203 / 7	pure shear	T5
20	Wörgler Klamm	Ladinian/Triassic	355000	260625	NDA	17	20 / 6	121 / 57	285 / 31	pure shear	T3
					NDA	5	123 / 71	5 / 8	272 / 15	pure shear	T4
21	Grattenbergl in Wörgl	Ladinian/Triassic	355950	262525	NDA	16	333 / 12	134 / 76	242 / 4	pure shear	T1
					NDA	6	277 / 2	178 / 72	8 / 17	pure shear	T5
					NDA	7	174 / 8	339 / 80	83 / 2	pure shear	T2
					NDA	8	226 / 29	32 / 59	133 / 6	pure shear	T3
22	Quarry “Anzen” in Brugger Mühle near Wörgl	Anisian/Triassic	356125	262500	kinematic interpretation	21	346 / 4	104 / 81	255 / 7	simple shear	T1
					NDA	9	162 / 5	252 / 1	355 / 85	pure shear	T1
					NDA	7	208 / 11	352 / 75	116 / 8	pure shear	T3
					Tension gashes	11			175 / 6	pure shear	T6
23	Quarry “Bergpeterl” south of Bad Häring	Rupelian/Oligocene	359000	262775	NDA	20	20 / 7	129 / 67	287 / 20	pure shear	T3
					NDA	15	342 / 23	144 / 65	249 / 6	pure shear	T4
					Tension gashes	12			292 / 3	pure shear	T4
26	Kössen: at 2nd bridge across Mosertalbach	Rupelian/Oligocene	381738	282418	NDA	9	204 / 16	93 / 49	306 / 35	pure shear	T3
27	E of Kössen: after 4th bridge across	Chattian/Oligocene	381875	282375	kinematic interpretation	4	33 / 16	226 / 72	124 / 3	simple shear	T3
					kinematic interpretation	4	136 / 3	26 / 80	227 / 9	simple shear	T1
28	Hacklriedgraben S of state road from Kössen	Rupelian/Oligocene	383000	280350	NDA	7	189 / 1	87 / 54	280 / 35	pure shear	T3
29	Kaiserwaldgraben SW Durchholzen	Chattian/Oligocene	368150	277775	NDA	14	350 / 6	247 / 63	83 / 25	pure shear	T1
30	Dirt road NE Großpoitneralm SSE Durchholzen	Anisian/Triassic	372350	276325	NDA	12	30 / 17	159 / 63	294 / 19	pure shear	T3
			372350	276325	NDA	6	36 / 67	209 / 22	300 / 2	pure shear	T4
			372350	276325	NDA	6	286 / 23	88 / 64	193 / 7	pure shear	T5
31	Arzler Alm S of Innsbruck	Anisian/Triassic	231010	240324	NDA	6	184 / 14	325 / 71	91 / 11	pure shear	T2
32	Rosnerweg in Mühlauer Klamm S of Innsbruck	Carnian/Triassic	231813	240254	NDA	8	189 / 16	336 / 71	91 / 11	pure shear	T2
34	NE Fraction Leiten of Achenkich	Late Triassic to Late Jurassic	254137	268668	NDA	13	174 / 9	81 / 16	293 / 70	pure shear	T2
					NDA	35	37 / 1	130 / 67	307 / 22	pure shear	T3
					NDA	11	98 / 10	192 / 20	342 / 66	pure shear	T5
					NDA	6	156 / 33	52 / 28	259 / 51	pure shear	T1
35	Quarry Kalkbruch S Bad Häring	Ladinian/Triassic	359469	263973	NDA	9	338 / 16	83 / 40	231 / 44	pure shear	T1
					NDA	6	197 / 71	0 / 18	92 / 5	pure shear	T4
					NDA	8	11 / 4	261 / 76	102 / 12	pure shear	T3
37	Blindau S of Reit im Winkel	Rupelian/Oligocene	385473	280134	NDA	8	221 / 2	115 / 79	312 / 9	pure shear	T3
38	Wasserfallgraben SE of Radfeld	Carnian/Triassic	343825	256775	NDA	13	31 / 40	201 / 49	297 / 5	pure shear	T3
39	Wöhler Graben NE of Hoheneiberg	Norian/Triassic	363755	266722	NDA	7	333 / 11	141 / 78	242 / 2	pure shear	T1
40	Wöhler Graben NE of Hoheneiberg	Rupelian/Oligocene	363755	266722	NDA	7	17 / 1	118 / 85	287 / 4	pure shear	T3
41	Wöhler Graben S of Hinterstein	Rupelian/Oligocene	364035	266877	NDA	10	213 / 3	334 / 83	123 / 5	pure shear	T3
					kinematic interpretation	14	348 / 3	92 / 76	257 / 13	simple shear	T1
43	Peppenau: Kitzwand N of Lengfeldenalm	Rupelian/Oligocene	362830	266502	NDA	12	30 / 12	160 / 71	297 / 13	pure shear	T3
45	Kaisergebirge: Jubiläumssteig E Gruttenhütte	Ladinian/Norian	373359	269028	NDA	16	327 / 15	118 / 72	235 / 08	pure shear	T1
46	Kaisergebirge: NW of Kaiser-Hochalm	Ladinian/Triassic	369788	269158	NDA	5	1 / 2	267 / 56	93 / 33	pure shear	T2
47	Kaisergebirge: Schneekar	Anisian/Triassic	370273	269388	kinematic interpretation	6	28 / 13	243 / 73	121 / 9	simple shear	T3
					kinematic interpretation	8	148 / 16	265 / 56	49 / 28	simple shear	T1
48	Kaisergebirge: Kreidegraben S of Griesenau	Norian/Triassic and Paleocene	377909	270542	Right Dihedra	10	0 / 6	244 / 74	91 / 13	pure shear	T2
49	Kaisergebirge: E of Wegscheid Hochalm	Anisian/Triassic	370753	268369	kinematic interpretation	8	143 / 17	307 / 72	52 / 4	simple shear	T1
50	State road from Kramsach to Brandenberg	Norian/Triassic	339673	259151	NDA	11	138 / 1	43 / 78	229 / 11	pure shear	T1
51	confluence of Mühlbach and Brandenberger Ache	Late Cretaceous	341814	263557	NDA	10	37 / 2	128 / 18	299 / 70	pure shear	T3
52	Western end of Kaisertal in Kufstein	Ladinian/Triassic	364175	273312	NDA	11	8 / 4	269 / 66	100 / 23	pure shear	T3
53	Schanzwände E Kufstein	Ladinian/Triassic	364120	273487	NDA	5	176 / 7	319 / 80	85 / 5	pure shear	T2
54	“Osterndorfer Finger” E of Bad Häring	Ladinian/Triassic and Rupelian	358879	264668	NDA	6	153 / 6	256 / 22	48 / 66	pure shear	T1
					Tension gashes	40			278 / 5	pure shear	T4
55	Lechtal Alps: N of Summit of Muttekopf	Campanian/Late Cretaceous	173957	236260	Direct Inversion	15	37 / 4	304 / 27	137 / 64	pure shear	T3

Table 1: Locations and results of paleostress analysis. Dataset 23 from Reiter (2000), 39-43 from Gruber (1995), 34 and 57-61 from Sausgruber (1994) and datasets 81-84 from Prager pers. comm. (2003).

No.	Location	Age of rock	X_{GKM} BMN	Y_M BMN	Method	N	σ_1	σ_2	σ_3	Geometry	Group
55	Lechtal Alps: N of Summit of Muttekopf	Campanian/Late Cretaceous	173957	236260	NDA	13	0 / 17	267 / 7	156 / 70	pure shear	T2
56	Lechtal Alps: Drischlsteig S of Muttekopfhütte	Campanian/Late Cretaceous	175946	235498	NDA	12	177 / 2	76 / 75	267 / 14	pure shear	T2
					NDA	7	8 / 62	143 / 20	240 / 17	pure shear	T4
57	Rofan: western face of Unnutz	early Late Cretaceous	254126	265707	NDA	9	171 / 2	261 / 2	33 / 86	pure shear	T2
58	Rofan: eastern face of Plickenkopf	early Late Cretaceous	252210	266334	NDA	8	328 / 0	58 / 9	234 / 80	pure shear	T1
60	Rofan: Pulverer Mahd N of Unnutz	early Late Cretaceous	256163	268297	NDA	12	346 / 7	78 / 8	217 / 78	pure shear	T2
61	Rofan: SW Festlalm Niederleger	early Late Cretaceous	255786	270413	NDA	6	40 / 5	131 / 15	291 / 73	pure shear	T3
					NDA	7	153 / 0	63 / 11	246 / 78	pure shear	T1
62	Lechtal Alps: E of Hanauer Hütte	Campanian/Late Cretaceous	170261	234521	NDA	8	162 / 4	70 / 20	263 / 69	pure shear	T1
63	Mitterbergtobel N of Bludenz	Carnian/Triassic	113452	226157	NDA	10	19 / 10	225 / 75	110 / 5	pure shear	T3
					NDA	5	158 / 23	251 / 7	358 / 64	pure shear	T2
64	dirt road across Muttersberg	Carnian/Triassic	112849	227236	Direct Inversion	7	37 / 28	206 / 61	305 / 4	pure shear	T3
					NDA	5	39 / 10	308 / 1	210 / 79	pure shear	T3
65	Mitterwald N of Bludenz	Carnian/Triassic	113019	225957	NDA	5	15 / 11	150 / 73	282 / 11	pure shear	T3
					NDA	6	163 / 8	295 / 77	72 / 9	pure shear	T1
66	W of Hahnenkamm summit near Reutte	Anisian/Triassic	173220	259694	NDA	7	134 / 21	41 / 7	292 / 67	pure shear	T1
					NDA	12	136 / 78	337 / 10	247 / 4	pure shear	T4
67	Stempeljoch NE of Innsbruck	Ladinian/Triassic	233789	243774	NDA	5	321 / 18	230 / 2	133 / 71	pure shear	T1
					NDA	7	250 / 69	39 / 17	132 / 9	pure shear	T6
68	Arlberg pass	-	140774	221169	NDA	8	342 / 5	189 / 83	72 / 2	pure shear	T1
					NDA		186 / 14	343 / 74	95 / 5	pure shear	T3
69	uppermost part of Lattenbach near Dawinalpe	Permoscythian	160519	223774	NDA	15	191 / 23	80 / 39	304 / 41	pure shear	T3
70	Flirsch	-	155895	223565	NDA	5	216 / 18	115 / 31	331 / 52	pure shear	T3
71	Kändlköpf W of Arlberg pass	Anisian to Ladinian/Triassic	137307	222132	NDA	8	0 / 1	264 / 78	90 / 11	pure shear	T2
72	Pontlatzer Brücke	-	174923	218724	NDA	13	342 / 19	168 / 70	73 / 1	pure shear	T1
					NDA	7	15 / 16	198 / 73	105 / 0	pure shear	T3
73	Puschlin	-	175782	219002	NDA	9	179 / 2	80 / 74	270 / 14	pure shear	T2
					NDA	10	321 / 11	203 / 66	55 / 20	pure shear	T1
74	N of Tunnel in Schnanner Klamm	Ladinian/Triassic	153592	224263	kinematic interpretation	10	150 / 11	275 / 71	57 / 11	simple shear	T1
75	N of Schnanner Klamm	Late Cretaceous	153326	224798	NDA	5	181 / 11	312 / 72	88 / 12	pure shear	T2
76	at state road E of Strengen	Permoscythian	162345	220987	NDA	7	329 / 12	173 / 76	329 / 12	simple shear	T1
77	W of Stanz near Landeck	Permoscythian	166152	223554	NDA	10	213 / 4	107 / 47	315 / 39	pure shear	T3
					NDA	12	196 / 22	62 / 58	295 / 20	pure shear	T3
78	Dalfazer Alm E of Maurach	Liasssic/Early Jurassic	256479	257516	NDA	6	352 / 81	178 / 8	88 / 0	pure shear	T4
					NDA	5	195 / 17	62 / 62	290 / 17	pure shear	T3
79	Ampelsbach	Jurassic	257764	271272	NDA	10	332 / 19	188 / 66	67 / 12	pure shear	T1
80	dirt road E of Rattenberg	Ladinian/Triassic	341986	256377	Direct Inversion	9	105 / 64	256 / 22	351 / 11	pure shear	T6
81	Fernpaß road at Hotel Fernstein	Norian/Triassic	186742	245393	kinematic interpretation	13	193 / 33	14 / 56	283 / 0	simple shear	T3
					NDA	12	347 / 33	249 / 10	144 / 53	pure shear	T2
					NDA	7	107 / 10	13 / 17	228 / 69	pure shear	T5
82	Römerweg above Hotel Fernstein	Norian/Triassic	187353	246315	NDA	5	176 / 11	343 / 77	86 / 2	pure shear	T2
					NDA	14	92 / 69	239 / 17	332 / 10	pure shear	T6
					NDA	7	0 / 13	268 / 6	152 / 74	pure shear	T2
84	Rauhes Tal W Fernpass	Norian/Triassic	186675	248198	NDA	10	53 / 56	252 / 61	147 / 8	pure shear	T3

Table 1 continued

events younger than Oligocene was established in Oligocene sediments using cross cutting relationships with the help of a discrimination matrix (Fig. 5d); this succession corresponds to the scheme by Peresson & Decker (1997a). Cross cutting relationships in rocks older than Oligocene were not systematic (Fig. 5a-c).

2.2.2 Deformational events and their ages

The observed stress tensors from old to young are:

T1: NNW-SSE contraction defined by conjugate strike slip faults and, less abundant, by thrust faults. On the large scale, thrusting within the NCA, of the NCA onto Penninic units and of the Alpine nappe stack onto the Molasse basin took place under NNW-SSE contraction.

T2: N-S contraction defined by conjugate strike slip faults and, less abundant, by thrust faults.

T3: NNE-SSW contraction defined by conjugate strike slip faults and, less abundant, by thrust faults. The only major shear zone in the investigated area, the Inntal shear zone was active during this event.

T4: E-W extension defined by conjugate normal faults. The direction of extension actually varies between WNW-ESE and WSW-ENE.

T5: E-W compression defined by conjugate strike slip faults and thrust faults.

T6: NNW-SSE extension defined by conjugate normal faults.

In the next paragraphs the characteristics, regional distribution and ages are discussed in more detail:

2.2.2.1 T1 (NNW-SSE-compression; Fig. 6)

The Oligocene deposits in the Inn valley are folded with WSW-trending axes on hecto- to kilo-

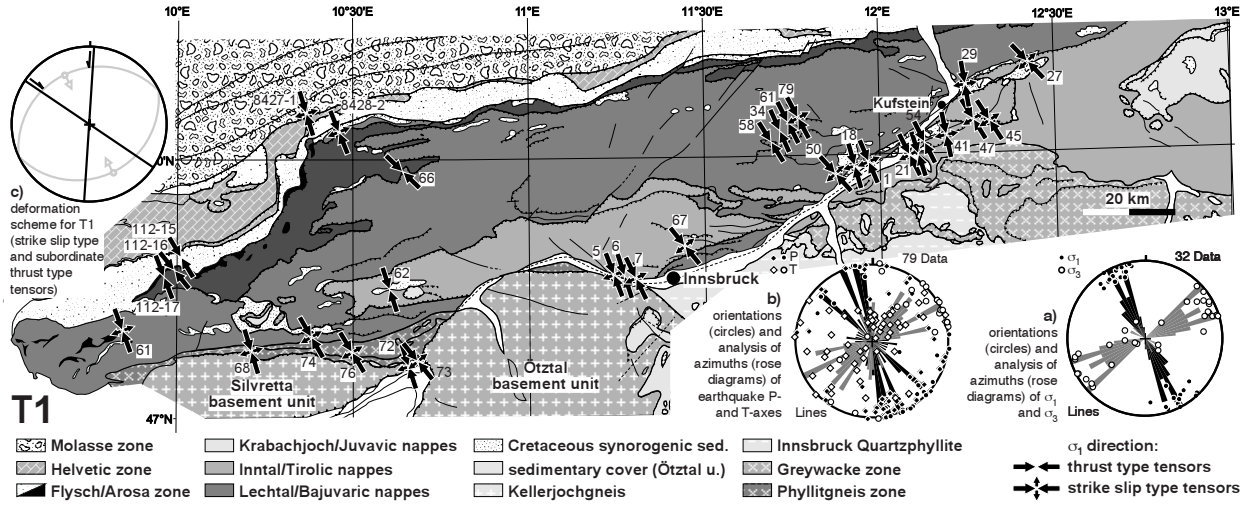

Fig. 6: Orientations of σ_1 (black arrows) of the tensor group T1 (NNW-SSE compression). Numbers next to arrows refer to Table 1 or to Decker et al. (1993) if >100. Inset a) orientations of σ_1 and σ_3 of all stress tensors of group T1 and orientation analysis of σ_1 (black rose diagram) and σ_3 azimuths (grey rose diagram). Inset b) orientation of compressional and extensional axes of earthquakes in the Alps and orientation analysis of P-axes (black rose diagram and T-axes (grey rose diagram). Data from Pavoni (1977)(circles) and Sleijko et al. (1987)(diamonds). Inset c) schematic representation of orientation of faults related to tensors of group T1.

metric scale (Fig. 4e & f). Conjugate dextral WNW- and sinistral N-striking faults are associated with folding and usually postdate folds. In all localities where T1 tensors were found in Oligocene rocks, NNW-compression led to formation of strike slip faults. In rocks older than Eocene, both strike slip faults and thrust faults are found, in some cases in the same station. In contrast to Peresson & Decker (1997a), who observed older thrust faults crosscut by strike slip faults in the eastern part of the NCA, no systematic succession could be deduced in the western part of the NCA. One reason is that D1 is heterogeneous:

- NW to NNW-directed contraction was active in the western part of the NCA during the Late Cretaceous, as demonstrated by Ortner (2001) in synorogenic deposits of the Muttekopf area. There, NW-striking dextral cross faults were active during NW-directed thrusting and folding (Fig. 6a,b; Eisbacher & Brandner, 1996), predating Late Cretaceous NNW-directed thrusting associated with folding of synorogenic sediments (l.c.; Fig. 7).
- NNW-directed shortening was active during deposition of Rupelian sediments on top of the NCA, as described in the chapter „Synsedimentary deformation".
- Post-Oligocene (Early Miocene) deformation caused folding and subsequent strike slip faulting in Oligocene sediments during NNW-directed compression, as described above (Fig. 4e,f). It did also affect the Molasse basin at the northwestern margin of the Eastern Alps (brittle data published by Decker et al., 1993; Schrader, 1988), which is clearly dominated by brittle structures related to NNW-SSE shortening (T1), orthogonal to the large fold trains of the allochthonous Molasse with regional WSW-ENE trending fold axes. The sediments of the allochthonous Molasse are Oligocene in age, and therefore the age of the faults must be younger than Oligocene. Also in the Flysch and Helvetic zones, D1 stuctures were frequently found.
- The orientation of P- and T-axes of earthquakes in the Alps (Pavoni, 1977; Sleijko et al., 1987; inset b in Fig. 6) parallel to σ_1 and σ_3 directions of T1 suggests, that NNW-directed contraction is still active. However, in the Oligocene deposits investigated, faults belonging to the T1 tensor group are systematically older than other faults (Fig. 5d).

When assuming the activity of cross faults during Cretaceous thrusting, a conceptual problem arises. Analysing brittle structures, usually an angle of 30° between fault plane and compressional axis is used. However, if interpreting NW-striking faults as cross faults, the angle between compressional force and fault plane is near 0° (Mandl, 1988). Therefore, most of the cross faults associated with NW-directed

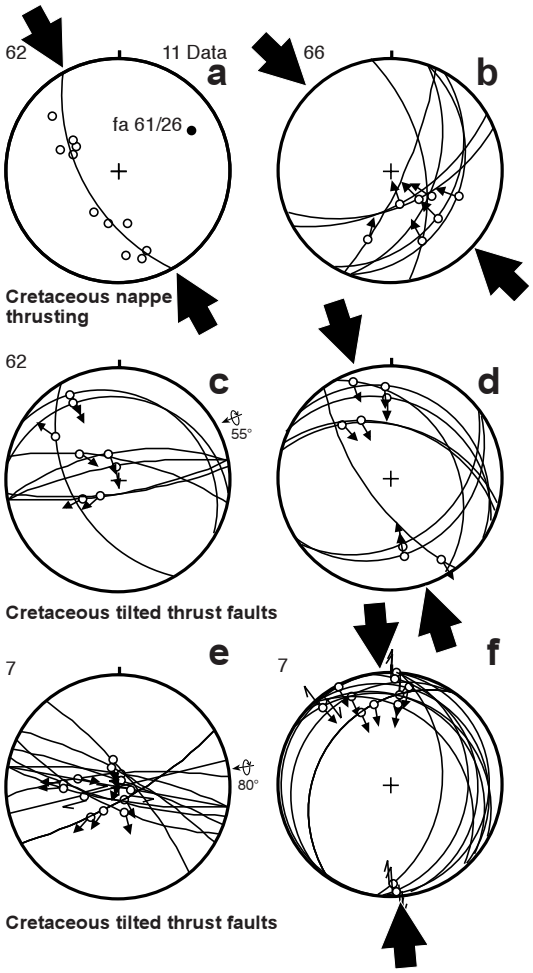

Fig. 7: Examples of Cretaceous deformation and the effect of later tilting. a) fold axis of fold sealed by Late Cretaceous sediments near Hanauer Hütte, Lechtal Alps. b) fault data set measured near the contact between Lechtal and Allgäu nappe near Reutte. c) Thrust faults from Late Cretaceous Gosau sediments associated with soft sediment deformation before backtilting and d) after backtilting. d) Thrust faults from the Triassic rocks before and d) after rotating with bedding back to horizontal around the regional fold axis.

thrusting will be attributed to NNW-SSE contraction, and only in the few cases, when the age of the fault and its relation to a thrust plane can be exactly defined, the interpretation will be correct. However, in this study NW- and NNW-directed compression are both part of the same tensor group T1, and the problem is avoided.

Nappe thrusting was postdated by folding. Fault data sets related to Late Cretaceous nappe thrusting should be tilted, except where the thrust plane is still horizontal. A few datasets of thrust type do show this geometry and can only be interpreted if rotated with bedding to a horizontal position (Fig. 7c-f). The identification of rotated cross faults is

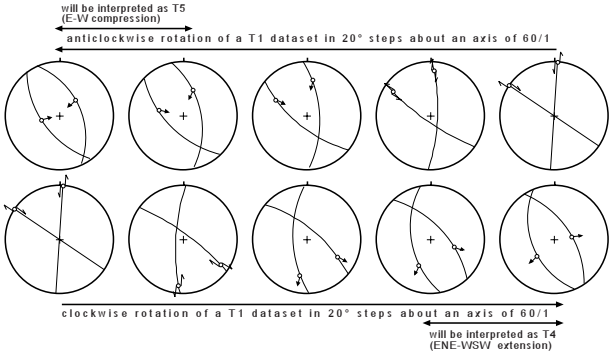

Fig. 8: The effect of tilting of strike slip datasets belonging to tensor T1. Top: anticlockwise rotation about a ENE-trending fold axis. If rotated more than ~60°, datasets will be interpreted to belong to tensor group T5 (E-W compression). Bottom: clockwise rotation about a ENE-trending fold axis. If rotated more than ~60°, datasets will be interpreted to belong to tensor group T4 (E-W extension).

more difficult, because tilted strike slip faults will be interpreted to be related either to E-W-extension or to E-W compression, if tilted to the opposite direction (Fig. 8).

2.2.2.2 T2 (N-S compression)

N-S compression was recorded in many stations in the western NCA, the Flysch, Helvetic and Molasse zones (Fig. 9). Both conjugate thrust and strike slip faults were observed. Where thrust faults were observed in Oligocene sediments, they are transitional to T3 (see below), otherwise conjugate NNW-striking dextral and NNE-striking sinistral faults were observed. No cross cutting relationships between thrust faults and strike slip faults were recorded. The age of N-S compression must be post-Oligocene, as Upper Oligocene sediments in the Molasse basin and in the Inneralpine Molasse are affected by this deformation. However, for older rocks, also a Late Campanian to Late Maastrichtian age of N-S compression must be considered, as suggested by Ortner (2001).

2.2.2.3 T3 (NNE-SSW-contraction)

An event showing NNW-SSE contraction was found in the NCA (Fig. 10). The western Flysch, Helvetic and Molasse zones were not affected by this event according to Decker et al. (1993). In a few

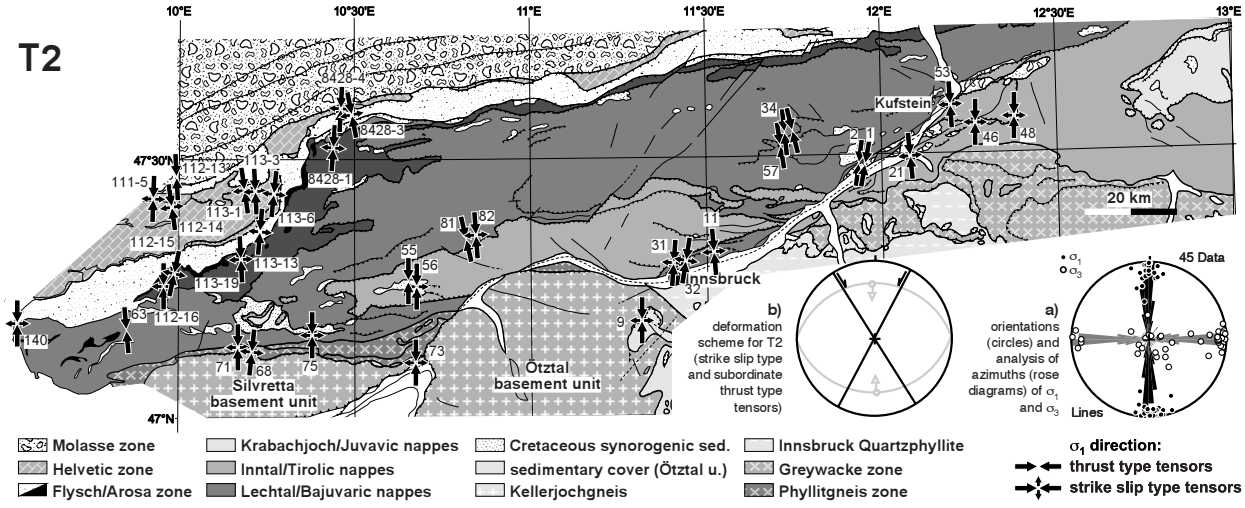

Fig. 9: Orientations of σ_1 (black arrows) of the tensor group T2 (N-S contraction). Numbers next to arrows refer to Table 1 or to Decker et al. (1993) if >100. Inset a) orientations of σ_1 and σ_3 of all stress tensors of group T2 and orientation analysis of σ_1 (black rose diagram) and σ_3 azimuths (grey rose diagram). Inset b) schematic representation of orientation of faults related to tensors of group T2.

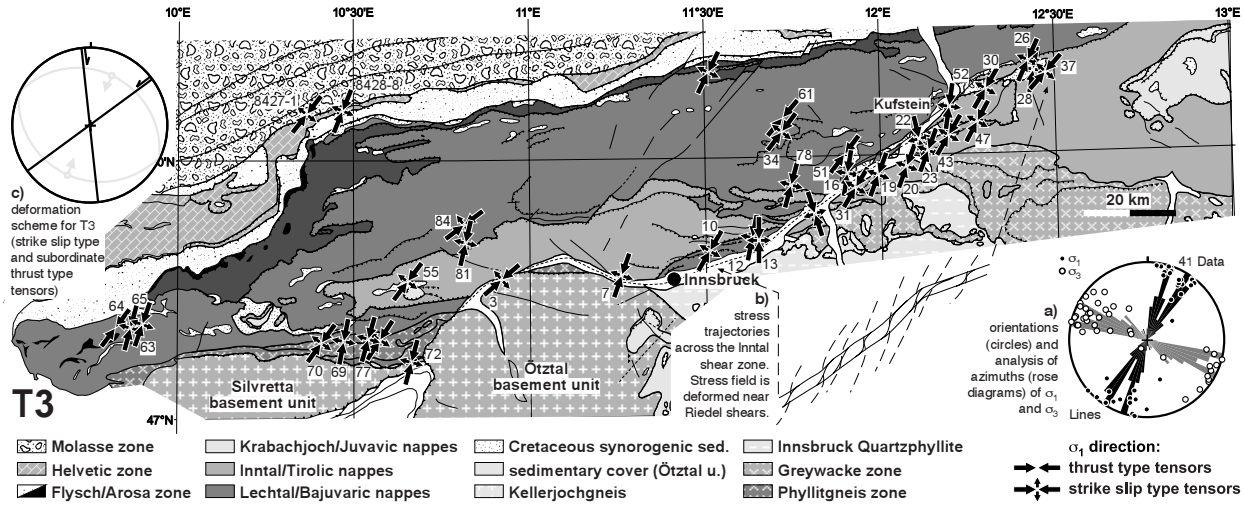

Fig. 10: Orientations of σ_1 (black arrows) of the tensor group T3 (NNE-SSW contraction). Numbers next to arrows refer to Table 1 or to Decker et al. (1993) if >100. Inset a) orientations of σ_1 and σ_3 of all stress tensors of group T3 and orientation analysis of σ_1 (black rose diagram) and σ_3 azimuths (grey rose diagram). Inset b) Schematic representation of deformed stress trajectories across the Inntal shear zone. Map scale Riedel shears within the shear zone lead to reorientation of the stress trajectories. Inset c) schematic representation of orientation of faults related to tensors of group T3.

cases conjugate reverse faults were observed, much more common are conjugate N-striking dextral and NE-striking sinistral faults. Due to their age and geometries two groups of faults must be distinguished:

- West of Innsbruck, usually conjugate fault sets, as described above, are found. On map scale, two sinistral fault systems can be traced in SW-direction from the front to the central part of the NCA: The Isartal and the Loisach fault systems (Fig. 1). Offset across the faults is in the range of 2 km for the Isar fault and probably in the same range across the Loisach fault. Both run into a zone of S-directed backthrusting (Eisbacher & Brandner, 1996). Following observations suggest a Paleocene/Eocene age of D3 west of Innsbruck:
  - In the Muttekopf area, subhorizontal NNE-directed thrusts crosscut folded Upper Maas-

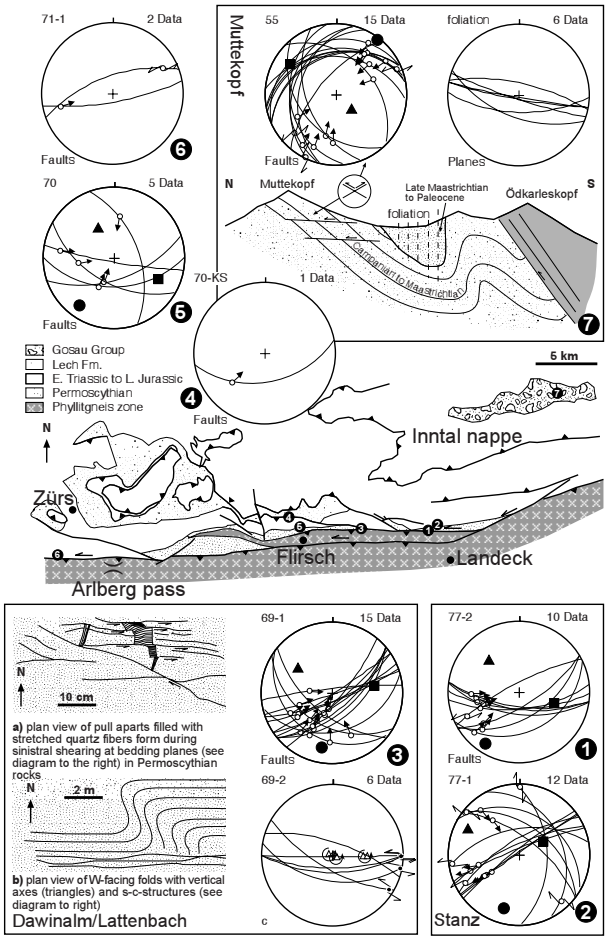

Fig. 11: Structural data from the Arlberg area illustrating NNE-directed contraction. Geological sketch modified from May & Eisbacher (1999). Inset "Muttekopf": Schematic N-S cross section across the Muttekopf Gosau outcrop showing post-Maastrichtian NNE-SSW contraction and associated foliation combined with brittle faulting. Inset "Dawinalm": a) formation of pull-aparts and b) folding with steep axes associated with bedding-parallel shear in Permoscythian rocks (diagram 3) and formation of s-c-structures in underlying phyllitic rocks (diagram lower right). Inset "Stanz": bedding parallel shear in Permoscythian rocks (diagram 2) and at the thrust beween Phyllitgneis zone and Permoscythian rocks (diagram 1).

trichtian to ?Paleocene sediments (Fig. 11, Inset „Muttekopf"; Ortner, 2001; the socalled „Deckelklüfte" of Niederbacher, 1982).

- In the Arlberg area, quartz fibres on steeply south dipping bedding planes in Permoscythian rocks (diagrams 1,2,3 of Fig. 11) and on similarly oriented foliation surfaces indicate NNE-SSW contraction. Shearing along the faults led to folding of bedding and foliation planes with subvertical axes and to formation of cm-size pull-aparts between shear planes (Fig. 11, inset „Dawinalm"). K/Ar ages from the area lie between 120 and 65 Ma (Thöni, 1981; Petschick, 1989). Rb/Sr ages from micas grown in the E-W-foliation show ages of 65 Ma (Ferreiro-Mählmann, 1994), suggesting a latest Cretaceous/Early Tertiary metamorphic event connected to formation of the foliation. The quartz fibres probably formed at the brittle-ductile transition during cooling in the Paleocene/Eocene.
- East of Innsbruck structures related to Oligocene/Miocene NNE-SSW compression are superimposed onto Paleocene/Eocene structures formed under compression in the same direction. In the Unterinntal Molasse, at the localities, where soft sediment deformation is observed, a mid-Oligocene age for D3 can be deduced , and a post-Oligocene age, where Oligocene sediments are affected by brittle faulting.

The fact that the NCA east of Innsbruck were affected by Paleocene/Eocene, Oligocene and Miocene NNE-contraction, which was alternating with NNW-contraction makes it evident, that cross cutting relationships cannot be systematic. It is still true, that most of the cross-cutting relationships indicate T3 younger than T1 (see Peresson & Decker, 1997a), however many indicate the opposite (Fig. 5). As it is not possible to distinguish between faults related to Paleocene/Eocene deformation and those related to Oligocene/Miocene deformation in rocks older than Oligocene/Miocene, the reversed successions may be a result of Oligocene/Miocene T1 faults overprinting Paleocene/Eocene T3 faults.

2.2.2.4 T4 (E-W extension)

The T4 tensor group is inhomogeneous, with extension directions ranging from WNW to WSW (Fig. 12; see also Peresson & Decker, 1997a). In most stations either conjugate normal faults or tension gashes are found. In the Unterinntal Molasse, fold axes in Upper Oligocene sediments consistently plunge to the WSW. Therefore the large scale normal faults are probably E-dipping. West of Innsbruck, ENE-WSW extension is locally found to be older than or alternating with T1, as observed in the Molasse basin (see Fig. 13 of Decker et al., 1993) and in Cretaceous sediments of the Muttekopf area (Fig. 13). The direction of extension in most of these data sets is parallel to the regional fold axis and is therefore interpreted to be related to extension

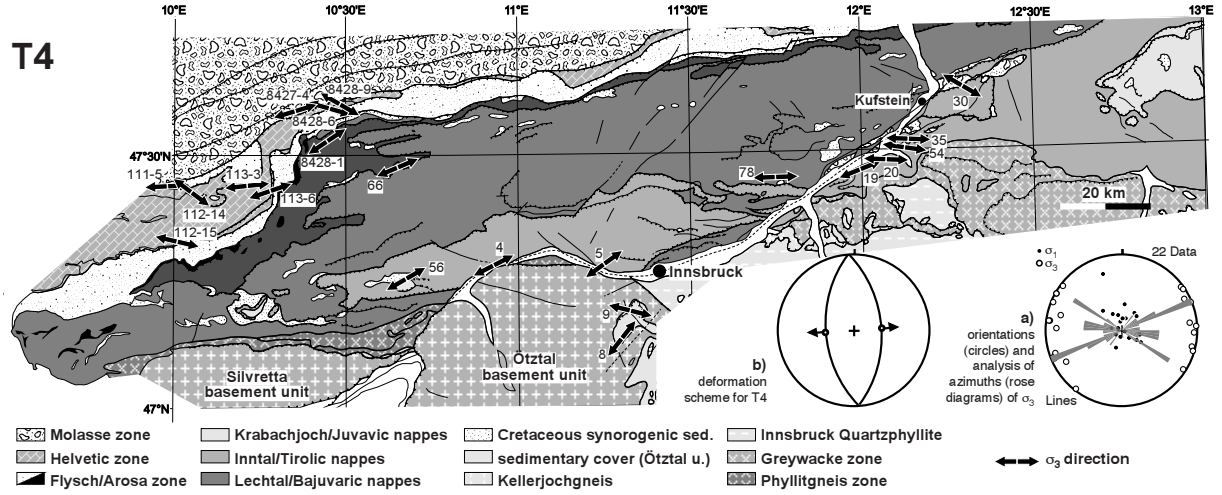

Fig. 12: Orientations of σ_3 (black arrows) of the tensor group T4 (E-W extension). Numbers next to arrows refer to Table 1 or to Decker et al. (1993) if >100. Inset a) orientations of σ_1 and σ_3 of all stress tensors of group T4 and orientation analysis of σ_3 azimuths (grey rose diagram). Inset b) schematic representation of orientation of faults related to tensors of group T4.

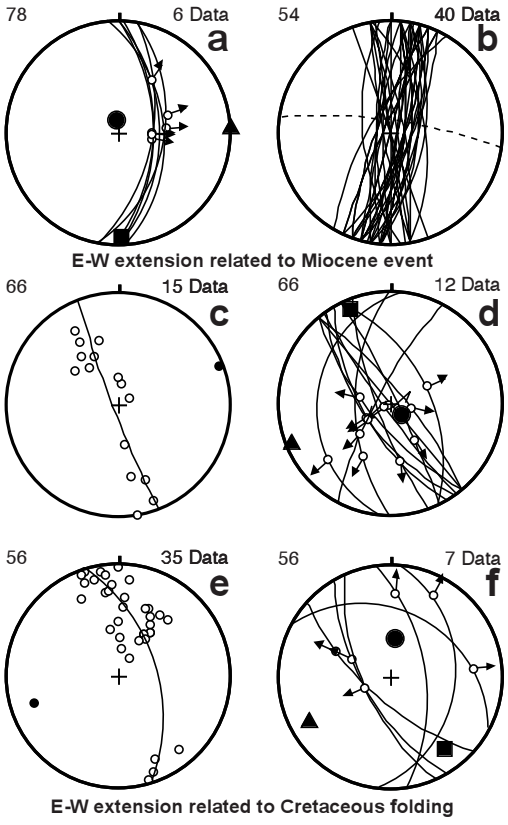

Fig. 13: Examples of data sets representative of E-W extension (T4). a) E-W extension recorded by fault planes, Dalfazer Alm, Rofan and by b) tension gashes in Oligocene carbonates, Bad Häring. c-f) poles of planes (white circles) and regional fold axis (black circle; left side) and fault data sets with σ_3 (black triangle) parallel to the fold axis. In this case, spreading of material parallel to the fold axis is interpreted. c) and d) from Triassic rocks at Hahnenkamm near Reutte, e) and f) from Drischlsteig near Muttekopf.

orthogonal to the direction of maximum compression.

2.2.2.5 T5 (E-W compression)

Throughout the investigated area, an event was recorded that reverses the movement sense of most of the major faults (Fig. 14). The analysis of these data sets consistently shows WNW-ESE compression. In outcrops, where no older steep faults are found, conjugate top-to-west or top-to-east thrust faults formed. Faults related to the T5 tensor are restricted to outcrop scale and do not create map-scale offsets. The age of this deformation cannot be constrained in the investigated area (except younger than Oligocene), however in the eastern part of the Eastern Alps it is also found in Middle Miocene rocks of the Ennstal Tertiary and the Vienna basin and has a Late Miocene age (Peresson & Decker, 1997b).

2.2.2.6 T6 (NNW-SSW extension)

In many outcrops, a conjugate WSW-striking set of normal faults is found, locally with offsets in the order of 100m (Fig. 15). Faults related to the T5 tensor group are restricted to the Inn Valley and the area immediately N of it west of Kufstein, and are found in the Flysch and Helvetic zones. This event is heterogeneous, because beside a Late Miocene age of activity as proposed by Decker et al. (1993), pos-

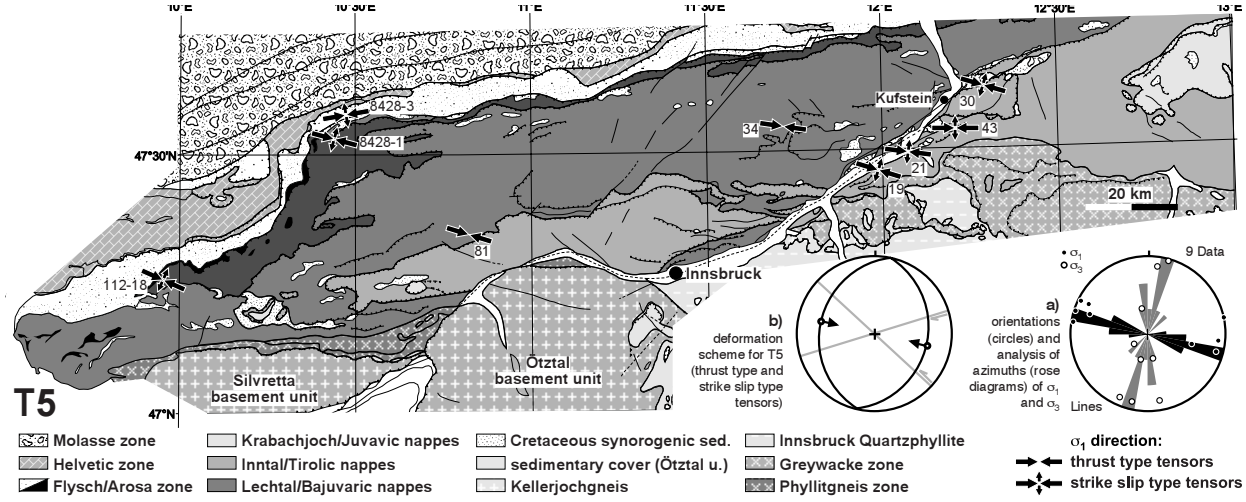

Fig. 14: Orientations of σ_1 (black arrows) of the tensor group T5 (E-W contraction). Numbers next to arrows refer to Table 1 or to Decker et al. (1993) if >100. Inset a) orientations of σ_1 and σ_3 of all stress tensors of group T5 and orientation analysis of σ_1 (black rose diagram) and σ_3 azimuths (grey rose diagram). Inset b) schematic representation of orientation of faults related to tensors of group T5.

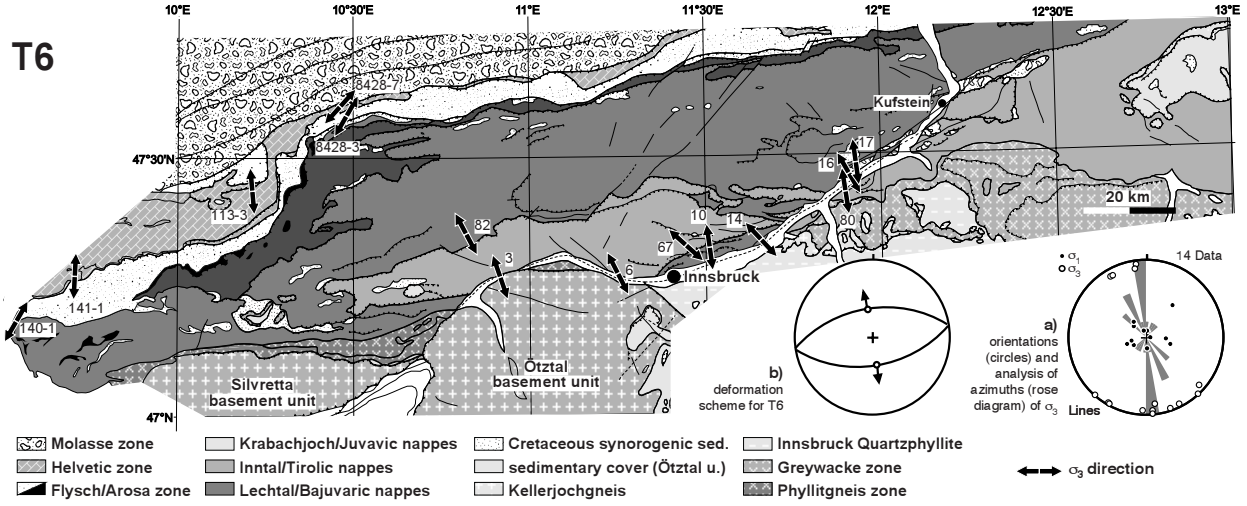

Fig. 15: Orientations of σ_3 (black arrows) of the tensor group T6 (NNW-SSE extension). Numbers next to arrows refer to Table 1 or to Decker et al. (1993) if >100. Inset a) orientations of σ_1 and σ_3 of all stress tensors of group T6 and orientation analysis of σ_3 azimuths (grey rose diagram). Inset b) schematic representation of orientation of faults related to tensors of group T6.

sible Cretaceous normal faulting during subsidence of Gosau basins (Wagreich & Decker, 2001) and Oligocene normal faulting, as discussed below, must be taken into account.

2.2.3 Activity of the Inntal shear zone

Faults related to the T3 tensor group are dominant in the Inn valley area, as T3 tensors are associated with shearing at the Inntal shear zone. Datasets from the T3 tensor group in this area often show simple shear geometry (see diagrams 16, 19, 25 of Fig. 16). The principal displacement zones in these datasets deviate from the orientation of the trace of the faults in map view, indicating that the master planes on outcrop scale are Riedel planes to the map scale faults. Therefore the maximum compressive stress within the shear zone is N-S to NNW-SSE directed. Datasets from within the shear zone can be distinguished from T2 datasets also indicating N-S compression by their simple shear geometry and from the position of the stations, where data were measured, on map scale Riedel shears (diagrams 22,29 of Fig. 16).

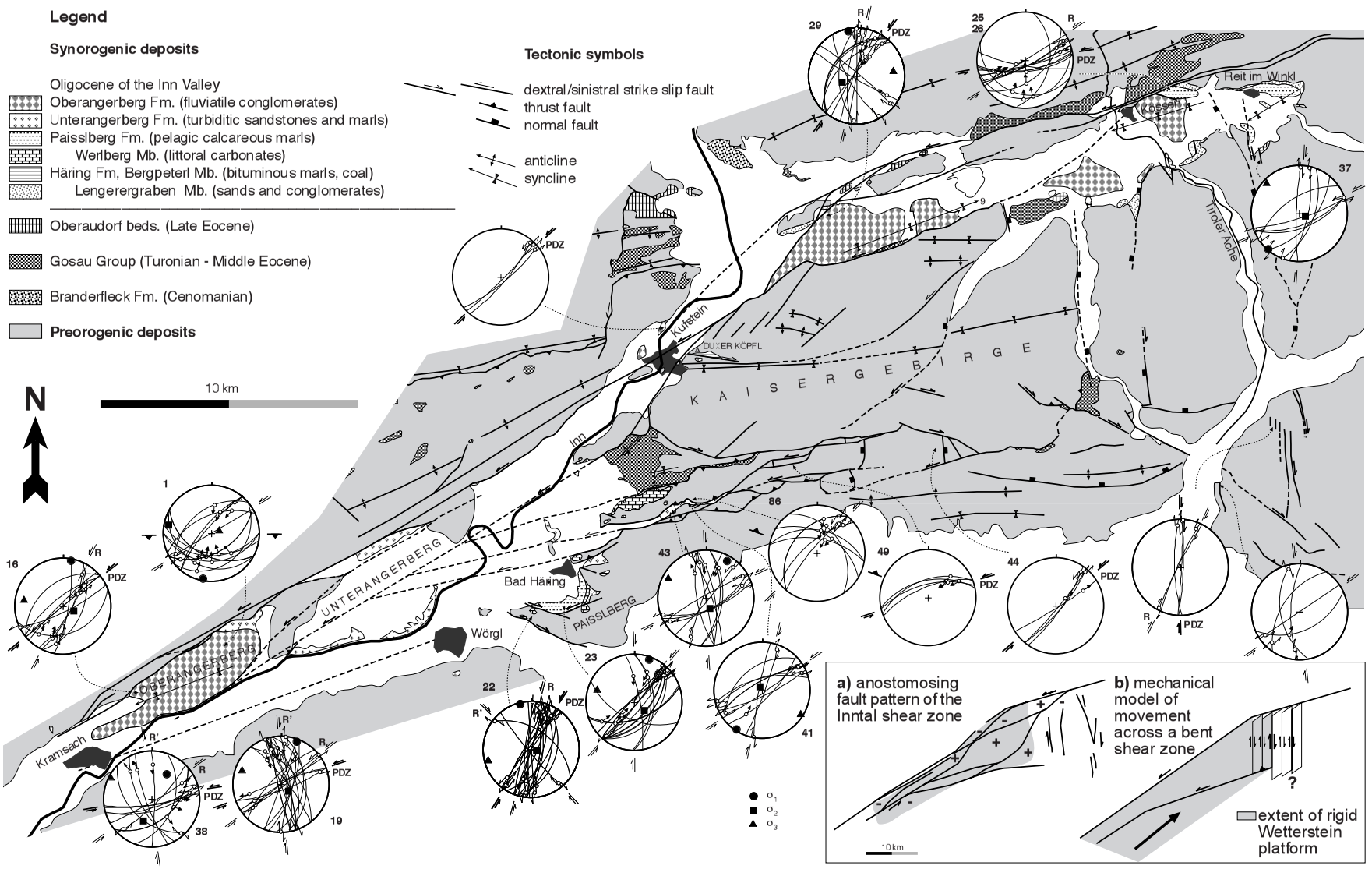

Fig. 16: Structural sketch of the Inntal Molasse and fault data sets illustrating shearing in the Inntal shear zone. Numbers next to diagrams refer to table 1. Inset a) shows the anostomosing character of the shear zone. The lozenge shaped blocks within the shear zone experienced either uplift (+) or subsidence (-) during shearing. Inset b) mechanical model for movement near the bend in the Inntal shear zone. Black arrow indicates assumed direction of movement parallel to western part of Inntal fault. PDZ = principal displacement zone. Further explanations in the text.

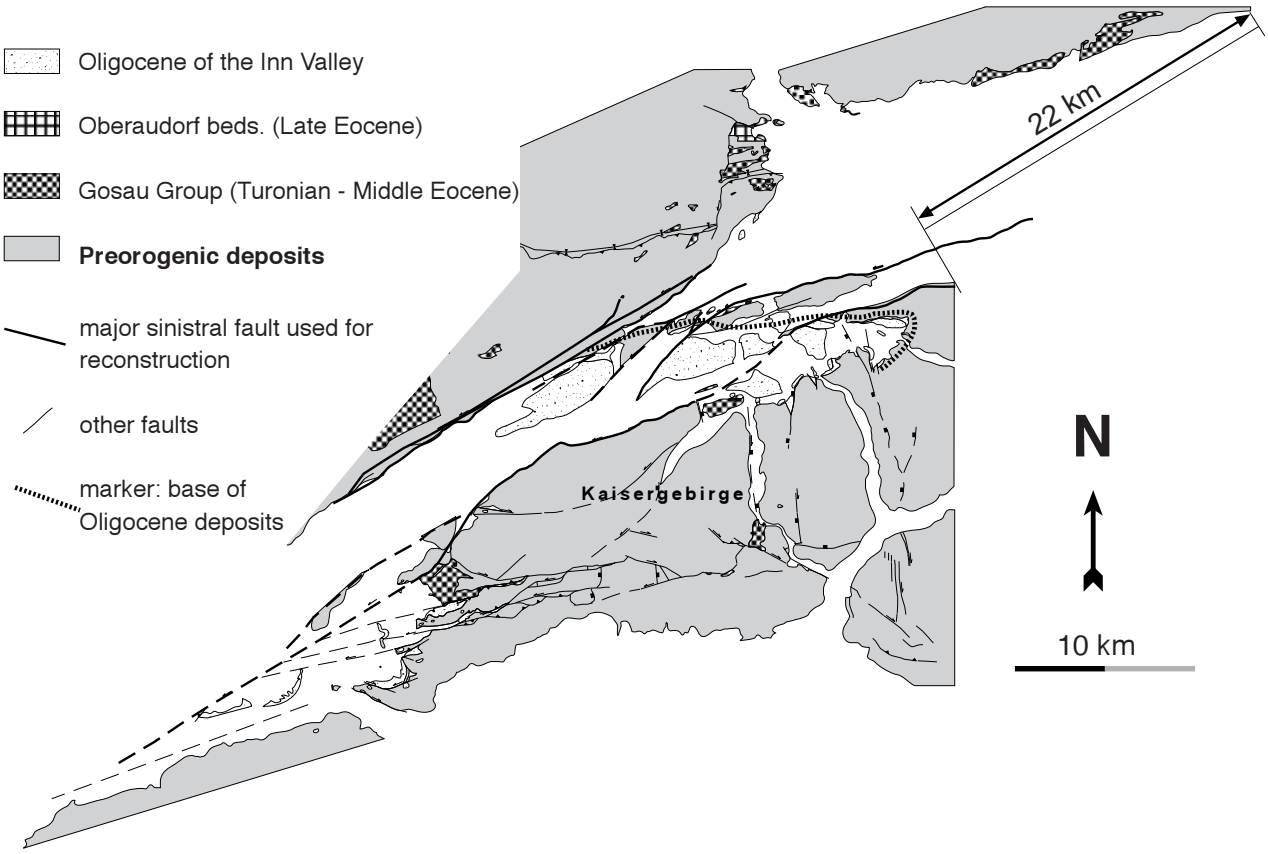

Fig. 17: Reconstruction of the pre-Miocene geometry of the Inntal. Due to the bended geometry of the Inntal shear zone, shortening orthogonal to the fault must increase toward the east. As the southern branch of the fault ends south of the Kaisergebirge, no major lateral offset was accomodated there.

2.2.3.1 Geometry of the Oligocene Inntal shear zone

From the begin of the latest Early Oligocene, debris from the eroding Alps was not transported across the Inntal shear zone toward the N, only the alluvial fan east of Kufstein did bring clasts from Australpine basement rocks into the Molasse basin (Ortner & Sachsenhofer, 1996; Brügel, 1998; Ortner & Stingl, 2001). Sediments were channelized along the Inntal shear zone to the Chiemgau fan. The Oligocene age of the swell is also proven by Upper Oligocene conglomerates in contact with Triassic rock north of the Inntal shear zone (Zerbes & Ott, 2000, cross section 14 on plate 2; Ortner & Stingl, 2003, this volume), that seal the relief created aong the Inntal line. Therefore Oligocene activity of the Inntal shear zone was combined with a normal throw of the southern block, as visible in Fig. 18 (see below). The data discussed in section 2.1 do not allow to decide, whether a shear zone with large offset existed in the Oligocene or not, but only confirm the existence of NE-SW compression in the Oligocene.

2.2.3.2 Geometry of the Miocene Inntal shear zone

In contrast, Miocene sinistral shearing is generally combined with S-directed oblique thrusting southwest of Kufstein and the Kaisergebirge, partly onto Oligocene sediments (Fig. 16, diagram 86; Gruber, 1997). This is probably an effect of a bend of the Inntal shear zone east of Kufstein from a strike direction of 54° to 71° (Fig. 16). Immediately east of the bend, a important component of shortening orthogonal to the fault (transpression) is indicated by curved fault planes changing alongstrike from thrust to strike-slip geometry (Fig. 16, diagram 25). Towards the east, the southdirected thrusts disappear and are replaced by N-striking dextral faults that dominate over ENE-striking sinistral faults and do show map-scale offsets (Fig. 16, inset a). This transition coincides with the eastern end of the Wetterstein carbonate platform. If the southern block moved parallel to the western part of the Inntal shear zone, movement across the bend will lead to major space problems. Therefore, near the south-

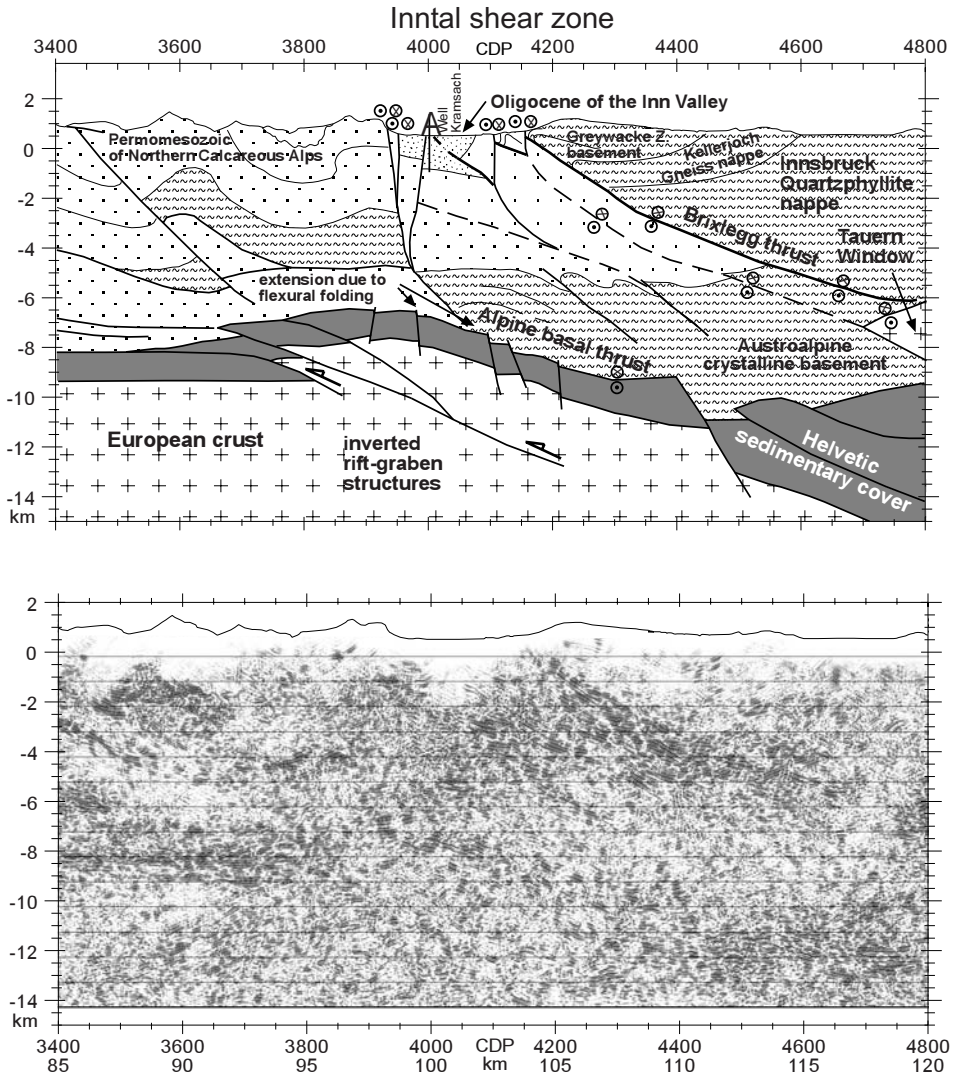

Fig. 18: Bottom: Depth-migrated TRANSALP section between km 85 and 120. Top: Geological interpretation of seismic transsect. Trace of section: 2 in Fig. 1.

ern margin of the carbonate platform, SE-directed thrusts developed . Further east, less rigid units were segmented into narrow units delimited by N-S-striking dextral faults, and shortening was transferred to the south (Fig. 16, inset b).

Within the Inntal shear zone, the Oligocene sedimentary succession was disrupted into lozenge shaped flakes and offset by ENE-striking sinistral faults. Under the assumption, that all lateral movements were horizontal and not combined with thrusting, as shown by the brittle data, the post-Oligocene offset can be reconstructed by bringing together the south-dipping northern basal contact of the Oligocene to older rocks. Depending on the sequence of activity of different branches of the Inntal shear zone, offsets between 22 and 30 km can be reconstructed (Fig. 17).

2.2.4 Thrust movements across the Inntal shear zone: interpretation of the TRANSALP line

The TRANSALP deep seismic line crosses the Inn valley near the westernmost outcrops of Oligocene rocks. A general interpretation of the TRANSALP seismic line was published by the TRANSALP working group (2002) (Fig. 2). They proposed a sub-Tauern ramp, cutting from the middle part of the European upper crust straight to the surface in the Inn valley, facilitating uplift and exhumation of the Tauern window. Near the surface, the NCA are overthrust by its basement. This upper part of the sub-Tauern ramp is renamed to Brixlegg thrust. The segment of the TRANSALP seismic line across the Inn valley was interpreted in detail by Ortner et al. (2003), to exactly define the place where the Brix-

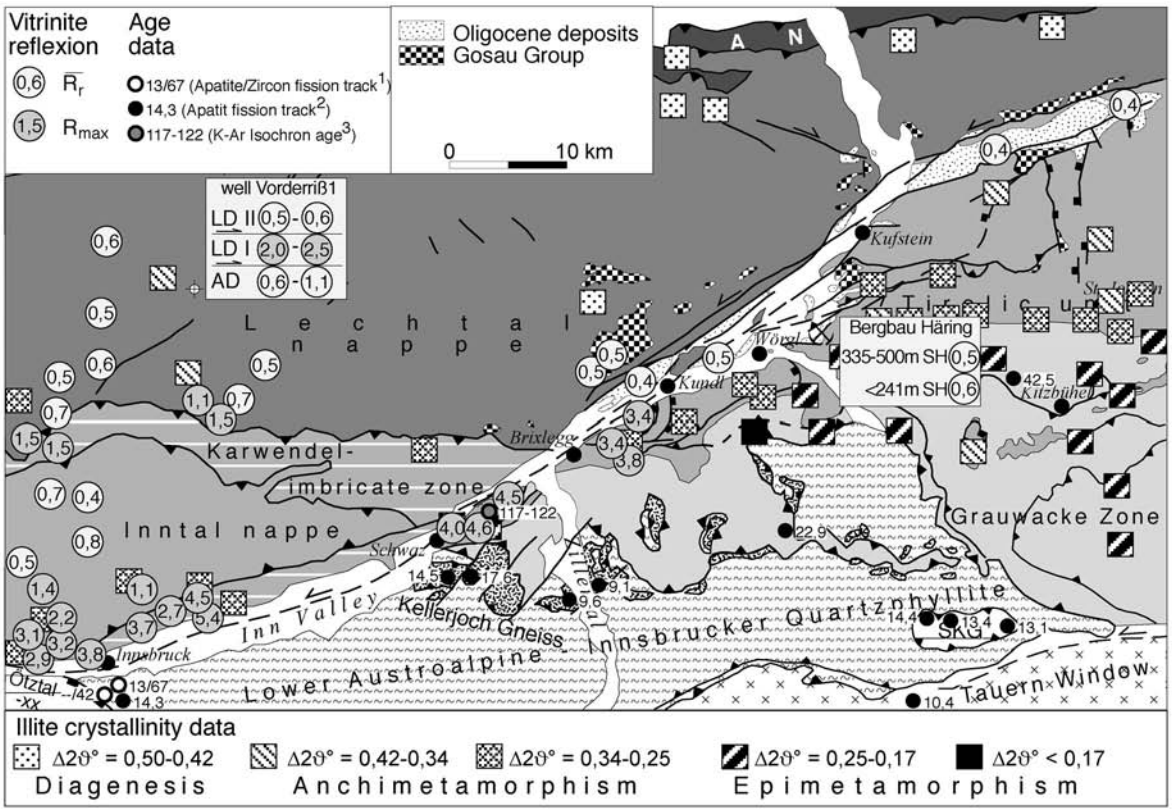

Fig. 19: Compilation of coalification data (Oligocene rocks: Ortner & Sachsenhofer, 1996; NCA: Petschick, 1989 and Reiter, 2000; well Vorderriß: Hufnagel et al., 1981), illite crystallinity data (Kralik et al., 1987), apatite and zircon fission track ages ([1]Fügenschuh et al., 2000; [2]Grundmann & Morteani, 1985) and a K/Ar isochrone age ([3]Krumm, 1984) from the NCA and southerly adjacent areas.

legg thrust reaches the surface and to evaluate timing and amount of displacement.

In the seismic section (Fig. 18), a contrast in reflectivity is observed across a plane dipping to the south from the southern margin of the Inn valley. Strong reflectivity is found below the plane, and the strongly reflective rocks continue to the north into the Northern Calcareous Alps. The pattern of reflections is comparable to the pattern created by the marls and dolomites of the Raibl Fm. found further north in the section (compare Auer & Eisbacher, 2003). Therefore a zone of imbricates or a very thick continuous section consisting of a succession of marls, dolomites and limestones is interpreted below the contrast. The weakly reflecting rocks above are part of the metamorphic basement of the Austroalpine unit, which in the section from top to bottom are the Greywacke zone, the Kellerjoch Gneiss nappe and the Innsbruck Quartzphyllite nappe (Fig. 18). The contacts between these units dip gently to the north, as does the foliation. The Greywacke zone is in sedimentary contact with the Tirolic unit of the NCA. The contrast in reflectivity is interpreted to represent a major thrust of the Greywacke zone and its sedimentary cover, the NCA and other basement units onto rocks of the NCA, the Brixlegg thrust.

The NCA in the hangingwall of the Brixlegg thrust experienced anchimetamorphic conditions during the Cretaceous (Rmax 3-4,5%; Reiter, 2000; Krumm, 1984; Fig. 19). Assuming no metamorphism in the footwall units of the thrust, a maximum vertical offset of 7-8km can be deduced, which is in line with the interpretation of the TRANSALP line in Fig. 18. Oligocene deposits overlie both the footwall and the hangingwall of the thrust. On the hangingwall, Oligocene sediments are widespread east of Kufstein and around Bad Häring, but disappear about 10 km east of the TRANSALP line. According to Kralik et al. (1987), anchimetamorphic conditions south of the Inntal shear zone are found as far to the east as Kössen and Reit im Winkl (Fig. 19). The anchimetamorphic rocks are overlain by Oligocene rocks that experienced only diagenetic conditions (Rr ~ 0,4%; Ortner & Sachsenhofer, 1996). Therefore most of the offset across the thrust is sealed by Oligocene sediments and must have a Paleocene/

Eocene age, as the thrust cuts Cretaceous nappe boundaries. However, the presence of solid bitumen in horsts within the basin indicates that some of the sediments reached the oil window, probably below the tip of the Brixlegg thrust (Ortner, 2003; Fig. 18). Minor (post-) Oligocene thrust movements are therefore interpreted. Towards the west, the young uplift related to the Brixlegg thrust increases, as seen on geologic map, because successively deeper units of the Cretaceous nappe stack are exposed in the hangingwall. Apatite fission track dating in the area south and east of Innsbruck revealed a phase of uplift around 14 Ma (Fügenschuh et al., 1997; Grundmann & Morteani, 1985) that might indicate the time of young thrusting (Fig. 19; see also Figs. 22,23), whereas Zircon fission track data scatter between 69 and 35 Ma. (Fügenschuh et al., 1997). According to these authors, this means that the rocks started to cool below 300° in the Early Paleocene. This is possibly related to Paleocene/Eocene uplift due to thrusting at the Brixlegg thrust.

In cross section, the Brixlegg thrust is offset by several south-side-up sinistral faults, which are part of the (Miocene) Inntal shear zone. This is the reason, that south of the Inn valley the footwall of the Brixlegg thrust cannot be observed at the surface (Fig. 18). At depth, the Paleocene/Eocene Brixlegg thrust must be deformed by the Miocene uplift of the Tauern window, however the Miocene activity of the thrust must be rooted in an antiformal stack below the Tauern window (Fig. 18; see also Fig. 22; Lammerer & Weger, 1998).

The sub-Tauern ramp must be connected to the Alpine basal thrust, because during uplift of the Tauern window in Oligocene/Early Miocene times, the frontal Alpine thust was still active, as pointed out by Lammerer & Weger (1998).

3 Discussion

As the NCA represent the topmost and northernmost part of the Austroalpine nappe stack, they did not experience significant metamorphic overprint except along their southern margin. Therefore all deformational events since passive margin formation adjacent to the Penninic ocean should be preserved and documented by brittle structures. As Jurassic deformation was accompanied by sedimentation, Jurassic structures were usually reconstructed using contrasting facies and thicknesses of Jurassic sediments (see Wächter, 1987; Channell et al., 1990, 1992; Lackeschewitz et al., 1991; Böhm et al., 1995; Hebbeln et al., 1996). Up to now, no analysis of brittle Jurassic faulting was done in the NCA. Jurassic deformation was characterized by normal faulting leading to development of horsts and grabens, which in some way were connected to strike slip faults, however the exact geometry of Jurassic faulting is not known in the investigated area. A tentative reconstruction was given by Channell et al. (1990), with NNE-strikung normal faults connected to ENE striking sinistral. At the western margin of the Austroalpine unit in eastern Switzerland, deformed Jurassic normal faults are well documented and are NNE-striking and both east and west-dipping in paleogeographic reconstructions (Froitzheim & Manatschal, 1996). There, normal faults were active throughout the Jurassic (l.c.). Recently, Gawlick et al. (1999) proposed Late Jurassic thrusting in the central part of the NCA based on a stratigraphic analysis and conodont alteration index (CAI) data, however no structural data were given to support the hypothesis.

3.1 Eoalpine thrusting

Thrusting in the Eastern Alps during the early Late Cretaceous is usually interpreted to be related to closure of the Meliata ocean, which was then located somewhere in the southeast of todays Eastern Alps (see paleogeographic reconstructions by Schmid et al., 1997 and Stampfli et al., 1998). The Adriatic plate, to which the Eastern Alps belong, was in a lower plate position at this time; the upper plate is still under dispute. According to Dallmeyer et al. (1998), thrusting propagated from the top to the base of the Cretaceous nappe stack in the eastern central part of the Eastern Alps between Cenomanian (ca. 95 Ma.) and the Maastrichtian (ca. 75 Ma.). In the western central part of the Eastern Alps, thrusting started later (Turonian; see review in Froitzheim et al., 1997; Trupchun phase). West-directed tectonic transport for this time span is well established (e.g. Froitzheim et al., 1994; Neubauer, 1987) in the Central Alps, even for the Greywacke zone (Ratschbacher & Neubauer, 1989), which is in sedimentary contact with the Tirolic nappe unit of the NCA. West-directed tectonic transport of nappes or slices within the NCA was reported only locally (e.g. Unnutz fold: Ortner, 2003), and nappe

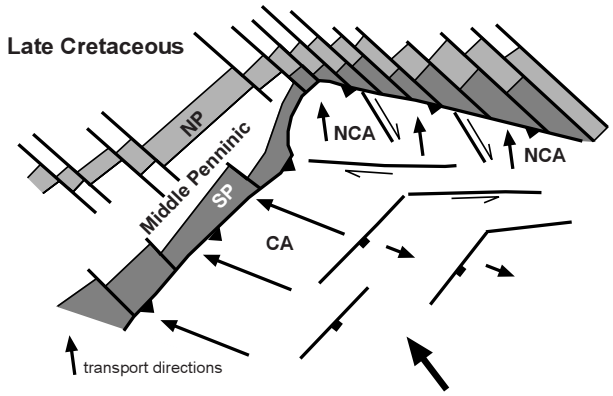

Fig. 20: Palinspastic model of the Alps in the Late Cretaceous following Schmid et al., (1997). Within the Eastern Alps, strain partitioning at approximately E-W striking faults caused diverging thrust directions in the Central Alps (CA) and Northern Calcareous Alps (NCA). Orogenic collapse leading to activity of major normal faults in the hinterland of active thrusting is delimited to the north by the same set of faults. NP = North Penninic ocean, SP = South Penninic ocean.

transport ssociated with folding was toward the NW (e.g. Eisbacher & Brandner, 1996) and NNW, as shown in this study. Ortner (2003) proposed a system of approximately E-W-striking faults along or near the southern margin of the NCA, across which WNW-directed thrusting could be partitioned into NNW-directed thrusting in the north and W-directed thrusting in the south (Fig. 20).

The basement units of the Eastern Alps were affected by extensional collapse caused by overthickening of the crust during preceding contraction. Major ESE-directed detachments were active (Silvretta unit: Froitzheim et al. 1997; Ötztal unit: Fügenschuh et al., 2000; Gleinalm: Neubauer et al. 1995) during west directed transport in the Campanian and Maastrichtian. This deformational phase is not found in the NCA. Instead, Campanian and Maastrichtian contraction was oriented N-S (Ortner, 2001). A possible reason for the change in the direction of compression in the NCA is the onset of extensional collapse in the central Alps, however the mechanism of strain partitioning is not clear at the moment. Late Cretaceous deformation is summarized in Fig. 20.

3.2 Paleocene/Eocene deformation

According to Eisbacher & Brandner (1996) and Froitzheim (1994) Paleocene/Eocene deformation was characterized by NNE-SSW compression. In the NCA, the Late Cretaceous synclines and anticlines are systematically offset by sinistral NE-trending faults. In the Central Alps, a dramatic change in transport direction took place since the Cretaceous, from W-directed to NNE-directed. The Austroalpine orogenic lid (in the sense of Laubscher, 1983) experienced not much internal deformation during the Cenozoic (Froitzheim, 1994), and also in the NCA only Cretaceous to post-Cretaceous sediments clearly do show folding due to Paleocene/Eocene contraction (Fig. 11; Fig. 2 in Eisbacher & Brandner, 1996). In other areas, continuing growth of prexisting fold structures has to be assumed. Paleocene/Eocene sinistral faulting across NE-striking faults cannot be related to possible continued extension in the central part of the Eastern Alps, as suggested by Froitzheim et al. (1996), because they end in S-directed (Isar- and Loisach faults; Eisbacher & Brandner, 1995, 1996) or N-directed thrust faults (Brandenberg; Ortner, 1996). Moreover, near the transition from the thick-skinned Central Alps to the thin-skinned NCA, a major thrust became active (Brixlegg thrust; BT in Fig. 21) and in its western continuation the Stanzertal fault in the Arlberg area (May & Eisbacher, 1999), which were the locus of major Paleocene/Eocene thrust activity (see section 2.2.1).

Onset of major out-of-sequence thrusting and therefore thickening of the orogenic wedge combined with sinistral faulting at the orogenic front

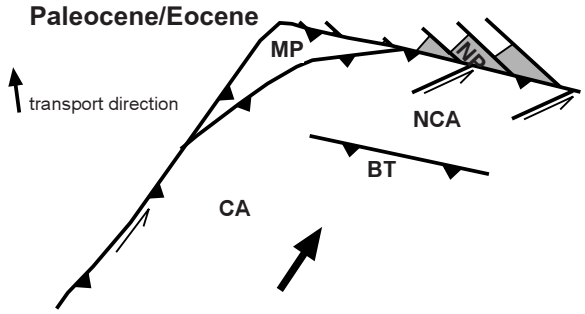

Fig. 21: Palinspastic model of the Alps in the Paleocene/Eocene modified from Schmid et al., (1997). Due to oblique collision with the distal European margin, sinistral NE-striking faults propagate from the front into the nappe stack and out-of-sequence thrusts within the Alpine wedge develop (BT = Brixlegg thrust). CA = Central Alps, NCA = Northern Calcareous Alps, NP = North Penninic ocean, MP = Middle Penninic unit.

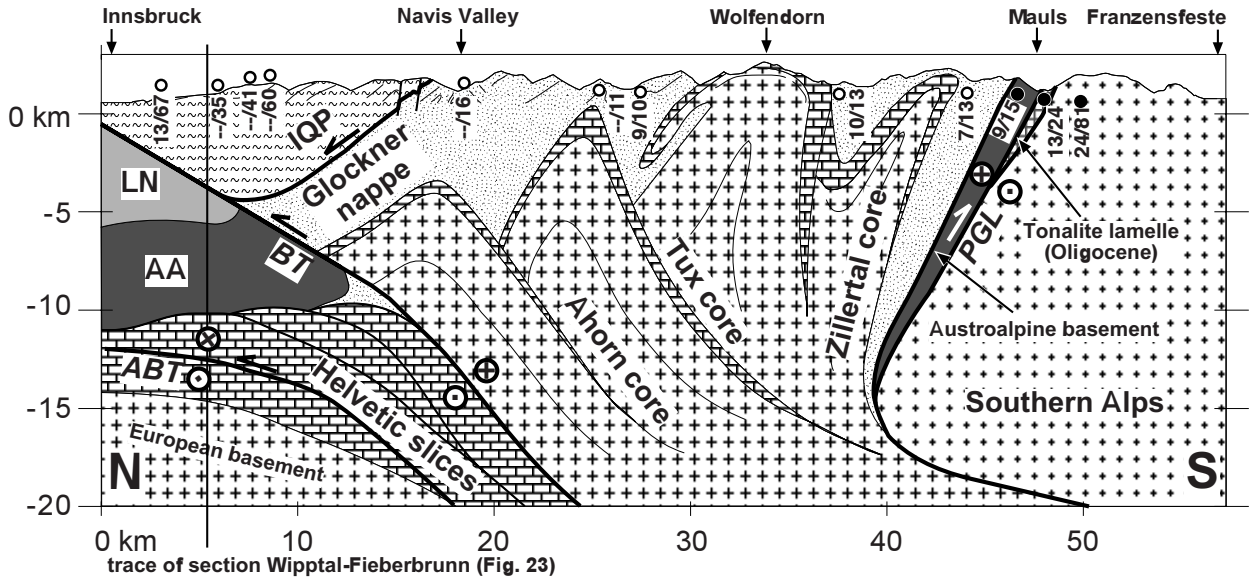

Fig. 22: N-S Cross section Innsbruck-Franzensfeste drawn using the results of the TRANSALP seismic section. Apatite and zircon fission track ages are indicated by symbols with numbers: white circles – Fügenschuh et al. (1997), black circles –Mancktelow et al., (2001). LN = Lechtal nappe, AA = undifferentiated Austroalpine basement, IQP = Innsbruck Quartzphyllite nappe, ABT = Alpine basal thrust, BT = Brixlegg thrust, PGL = Pustertal-Gailtal line. Trace of section: 2 in Fig. 1.

could possibly be related to oblique collision with the most distal part of the European margin. This is for example documented in the duration of flysch sedimentation in the Rhenodanubic Flysch, which ends in the Maastrichtian in the west (Vorarlberg; Tollmann, 1985) and in the Early Eocene further east (Salzburg; Egger, 1992). Paleocene/Eocene deformation is summarized in Fig. 21.

3.3 Oligocene/Middle Miocene deformation east of the Brenner normal fault

The main processes within the Alps controlling Oligocene/Miocene deformation are:

- collision of the Adriatic plate with the European margin and accretion of flakes of this margin into the Alpine edifice. The European distal margin was overthrust after the Bartonian (late Middle Eocene), as the youngest sediments in the Ultrahelvetic unit at the Alpine front have this age (Hagn, 1981). Sedimentation on the Helvetic margin lasted until the Priabonian (Late Eocene; l.c.). At the same time, basement slices were scraped off the European margin to form an imbricate stack in the area of todays Tauern Window, which was tilted to the south as the basal thrust propagated downward (Fig. 22).
- ductile orogen-parallel stretching below the Brenner and Katschberg normal faults (Ratschbacher et al., 1991; Fügenschuh et al., 1997; Frisch et al., 2000), which was contemporaneous with stacking of horses and exhumation of the Tauern Window (Lammerer & Weger, 1998) and major backthrusting along the Periadriatic line.
- formation of a peripheral foreland basin at the end of the Eocene.

These processes are the frame, in which the brittle processes in the NCA must be seen. Especially orogen-parellel extension in the Tauern window is seen as a controlling factor on brittle deformation in the NCA and is therefore dicussed here in some detail:

3.3.1 Oligocene/Early Miocene

Following Fügenschuh et al. (1997), exhumation of the Tauern window took place in two stages: Prior to 13 Ma, only the Penninic Tauern Window was in the footwall of the Brenner normal fault, and Austroalpine units north of it were in the hangingwall, so that most of the relative movement inbetween must have been transferred into the northern margin of the Tauern window, and further east into the SEMP-line Fig. 1). Moreover, the roof of the Tauern window must have been relatively flat, as it is still today (see cross sections of Thiele, 1976). Due to the drag of the eastward moving Penninic units a

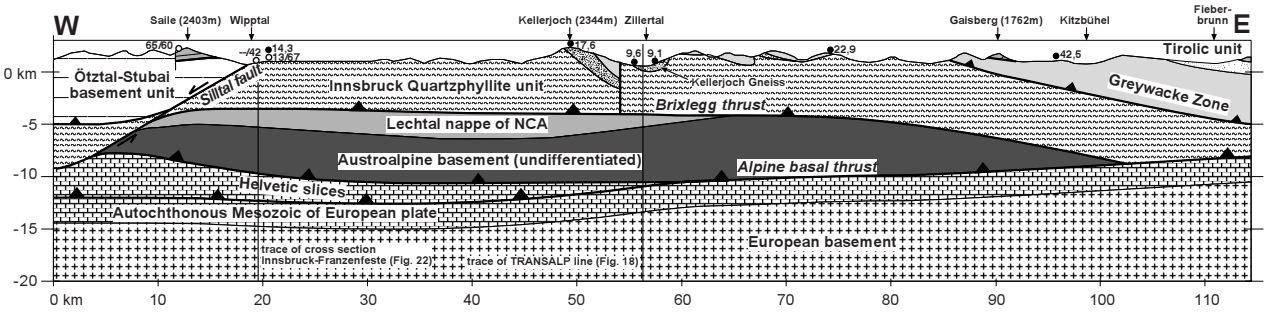

Fig. 23: E-W Cross section Wipptal-Fieberbrunn drawn using the results of the TRANSALP seismic section. Apatite and zircon fission track ages are indicated by symbols with numbers: white circles – Fügenschuh et al. (1997), black circles – only apatite fission track ages, Grundmann & Morteani (1985). Trace of section: 3 in Fig. 1.

secondary stress field developed north and on top of the Brenner normal fault, leading to a reorientation of the maximum compressive stress from NNW-SSE to NNE-SSW, as outlined already by Decker et al. (1994) for Miocene times. At the Inntal shear zone, no major sinistral offset due to exhumation of the Tauern window is expected, but rather NNE-directed contraction combined with sinistral shearing, as observed (see section 2.1).

The normal fault component across the major sinistral faults cannot be understood in this scenario. On orogen scale, the latest Eocene and Early Oligocene was the time, when the Alpine foreland basin subsided rapidly (e.g. Zweigel et al. 1998) due to flexure of the European plate. As shown by Ortner & Stingl (2001), on top of the NCA a piggy back basin formed, which was part of the Molasse basin during the Oligocene. Strong subsidence in the area of the NCA requires that most of the load was located to the south. The load was most probably created by out-of-sequence thrusting and thickening of the Alpine wedge in todays Tauern Window after increase of friction at the base of the wedge related to the arrival of buoyant European continental lithospere in the subduction zone. In the Molasse basin, a system of approximately WNW-ESE-striking normal faults formed, sealed during sedimentation in the Molasse basin, which are both hinterland and foreland-dipping (e.g. Figs. 2, 4 and 5 of Bachmann et al., 1982; Zweigel et al., 1998; plate 1 of Brix & Schultz, 1993) and formed due to bending stresses during flexure of the lower plate (see p. 203 in Price & Cosgrove, 1990). A possible nucleus of the Inntal shear zone could be such a hinterland-dipping normal fault, rooted in the European plate.

3.3.2 Middle Miocene

Via the Wipptal fault (Fig. 1), the approximately N-S trending Brenner normal fault is connected to the sinistral ENE-striking Inntal shear zone to the north. This is a result of Miocene activity of the Brenner normal fault after 13 Ma (Fügenschuh et al., 1997), when the Innsbruck Quartzphyllite unit was part of the footwall of the Brenner normal fault, which was then extending to the Inn valley in the north and called Wipptal fault. Vertical offset across the Wipptal fault was in the range of 4-5 km (l.c.), leading to a sinistral offset across the Inntal fault of about 8.5 km, assuming a dip of the Wipptal fault of 30°, or 9 km assuming a dip of 25°. Exhumation of the Innsbruck Quartzphyllite was not only due to east-directed upward movement below the Wipptal fault, but also due to synchronous thrusting at the Brixlegg thrust and other related thrusts (Fig. 23). Thickening of units is needed to fill up the space created by uplift of the Innsbruck Quartzphyllite nappe.

Sinistral shearing along the Inntal shear zone in Middle Miocene times is part of the lateral extrusion in the sense of Ratschbacher et al. (1991). The TRANSALP cross section (Fig. 18) offers the opportunity, to examine the 3D-geometry of lateral extrusion in its westernmost part. Ductile E-W extension in the Tauern window took place between the S-dipping Alpine basal thrust and/or the Brixlegg thrust in the N and the N–dipping oblique dextral backthrust of the Pustertal-Gailtal line due to strong compression in front of the indenter of the Southern Alps (Fig. 22). Sinistral faulting across the Inntal shear zone delimited the eastward movement

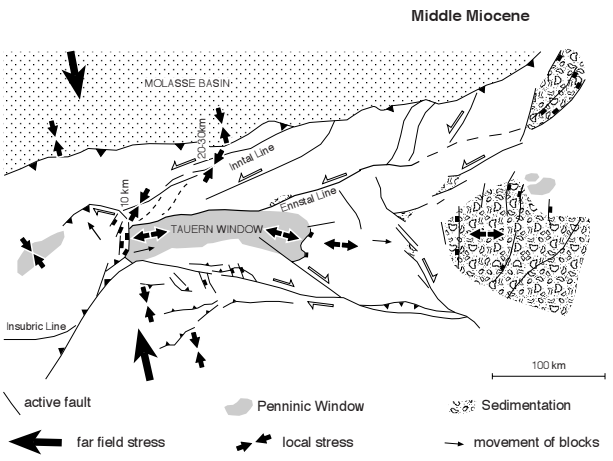

Fig. 24: Palinspastic reconstruction of the Eastern Alps and Southern Alps for Middle Miocene during orogen-parallel extension and sinistral shearing at major faults with directions of local stress indicated in different regions of the Alps. Dashed line S of the Inntal line indicate hypothetical faults needed to transfer sinistral offset from the Tauern window northern margin to the Inntal line, because of the eastward increasing offset, indicated by numbers north of the Inntal line.

of the units to the south of the Inntal shear zone toward the N.

As shown in this paper above, during the Oligocene/Miocene NNW-SSE contraction and NNE-contraction related to sinistral faulting were alternating in the southern part of the NCA, controlled by processes in the metamorphic core complex of the Tauern window. NNW-SSE contraction is observed in the NCA, when thickening was dominating over E-W-extension in the Tauern Window metamorphic core complex. This contraction corresponds to the far field stress as in the Molasse basin (Schrader, 1988) and in the Southern Alps (Castellarin & Cantelli, 2000; Fig. 24). NNW-SSE contraction prevailed during times of orogen parallel extension, in the Eastern Alps. When extension dominated over contraction, a secondary stress field with NNE-SSW direction was imposed on all units to the north (Fig. 24).

3.3.3 Oligocene/Middle Miocene deformation west of the Brenner normal fault

West of the Brenner normal fault, Oligocene/Miocene NNE-compression did overprint structures related to Paleocene/Eocene deformation only weakly, and no map-scale sinistral faults with large offset are known. However, the crosscutting relationships between outcrop scale faults belonging to datasets related to NNW-contraction and NNE-contraction are not systematic as well (Fig. 5b), suggesting another phase of NNE contraction in this area as well. Ratschbacher et al. (1991) proposed NNW to NW contraction west of the Brenner line during lateral extrusion. The Domleschg phase of Froitzheim et al. (1994) probably represents this contraction which may also account for some brittle structures in the NCA.

The main Oligocene/Miocene structures south of the NCA are the Engadine Window, another window of Penninic units within the Austroalpine basement, and the Engadine line (Fig. 1), which was active during exhumation of the Engadine window (Froitzheim & Schmid, 1993; Schmid & Haas, 1989; Pfiffner & Hitz, 1997). Like the Tauern window, the Engadine window was exhumed by the stacking of European basement slices during the Late Oligocene/Early Miocene. The Engadine line acted as normal fault at the the eastern side of the window and offset the Ötztal basement unit against the Penninic units by 4 km in response to passive backthrusting above a Helvetiv basement slice actively thrusting toward the NW (Hitz & Pfiffner, 1996). Therefore no regional extension is needed for normal faulting across the Engadine line. Synchronous uplift at the western block at the southern end of the Engadine led to block rotation along the Engadine line. As the pole of rotation was located below todays earth surface, sinistral movements are observed in the central part of the Engadine line (Schmid & Froitzheim, 1993).

Probably more relevance for deformation within the NCA has the Turba phase at the western margin of the Eastern Alps. The Turba normal fault (Fig. 1) downthrows the Lower Austroalpine Platta nappe against Penninic flysch units approximately 2 km to the east (Nievergelt et al., 1996). Weh & Froitzheim (2001) described a northern continuation of the Turba normal fault, the Gürgaletsch shear zone, which ends in the Prättigau half-window.

Phases of extension in the Central Alps could lead to the modification of the stress field (NNW-SSE contraction) in the hangingwall of the normal faults, where extension will prevail and to the north of the extending region, where extension must be delimited by steep faults against stable regions. Both events could lead to a (re)activation of sinistral E(NE)-striking steep faults in the NCA and therefore to creation of a secondary NNE-SSW oriented contraction.

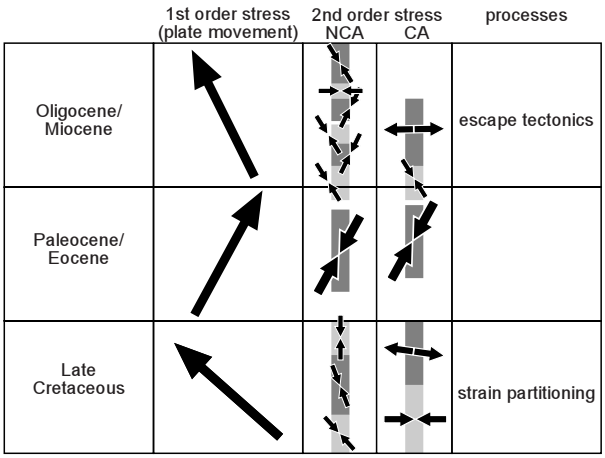

Fig. 24: Attempt to correlate deformational structures in the NCA and in the Central Alps. Data from Central Alps taken from Froitzheim et al. (1997) and Lammerer & Weger (1998). NCA = Northern Calcareous Alps, CA = Central Alps.

3.4 Late Miocene

Late Miocene E-W compression is found in various locations within the investigated area and was also described by previous authors (e.g. Müller-Wolfskeil & Zacher, 1984). Peresson & Decker (1997b) relate this stage of deformation in the eastern part of the NCA to continental collision in the eastern Carpathians. This event reactivates many older fault planes, but does not create map scale structures.

3.5 Post-Miocene

NNW-SSE extension is mainly found in and near the Inn Valley. Similar normal faults have been related by Decker et al. (1993) and Peresson & Decker (1997a) to gravitational collapse due to ongoing uplift of the Alpine chain. An alternative model is related to the interpretation of the TRANSALP seismic section. The basal reflections below the Molasse basin, which are related to the Jurassic-Cretaceous sedimentary succession of the autochthonous Mesozoic, can be traced horizontally to the south under the NCA until some point below the Inn valley in a depth of 8 to 9 km (Fig. 18). Near the end of the throughgoing reflections, a similar set of reflections, frequently interrupted, downlap on the latter and continue via a open anticline into well-defined reflections, which clearly represent the autochthonous Mesozoic in a depth of 12 to 14 km. The structure inbetween is interpreted to be an inverted Cenozoic rift graben structure (Fig. 18). Its formation and growth after the end of major thrusting at the Alpine basal thrust could well have led to normal faulting above, caused by extension above a neutral surface during flexural folding. This type of faulting is restricted to the locus of the fold in the subsurface (see Fig. 15). In other places, normal faulting might be older and for example related to Early Oligocene normal faulting during flexure of the European plate (see section 3.3.1) or Cretaceous normal faulting as described by (Wagreich & Decker, 1991).

4 Conclusions

Brittle deformation recorded in the western part of the NCA can be related to distinct events of Alpine orogeny:

- Eoalpine thrusting (after Hauterivian) was responsible for initial nappe stacking in the NCA and created folds with NE-trending axes and NW-striking cross faults. Subsequent NNW-SSE contraction led to folding of thrusts and formation of many of the main folds within the NCA. Strain partitioning across (hypothetic) approximately E-W-striking shear zones might be responsible for diverging thrust directions in the NCA (top to NW to NNW) and Central Alps (top to W). Deformation took place in a lower plate position in relation to closure of the Meliata-Hallstatt ocean.

  Strain partitioning created local stress fields on both sides of shear zones. Therefore both E-W-compression in the Central Alps and NNW-SSE compression in the NCA have to be considered as local stress fields. The true orientation of the far field stress cannot be deduced from field data, but must lie between the orientations of compression in NCA and Central Alps.
- Paleocene/Eocene deformation led mainly to fold growth of prexisting folds and formation of new folds with WNW-trending axes. Some larger NE-striking faults propagagated from the front of the Alpine wedge toward the south. A first set of major thick-skinned out-of sequence thrusts like the Brixlegg thrust developed. The reason was oblique collision with the distal European margin.

  During the Paleocene/Eocene, no major differences regarding the direction of compression between different units in the Alps could be

observed. Therefore, NNE-compression is thought to be represent the far field stress.

- Post-collisional Oligocene/Miocene deformation was characterized by major out of sequence thrusting and thickening in the central part of the Alps combined with orogen parallel extension and eastward escape of crustal blocks. Eastward movement took place between N- and S-dipping out-of-sequence thrusts. The analysis of brittle data in the NCA showed, that the process must have been episodic. There, alternating phases of NNW-SSE compression and sinistral shearing at the northern margin of eastward escaping blocks were recorded. The tensors indicating NNW-SSE-directed compression are regarded to represent the far field stress, whereas a secondary stress field with NNE-SSW oriented compression was created by the drag of eastward moving blocks during phases of dominant extension. NNW-directed compression is still active, as the orientation of compression axes of earthquakes indicate (Fig. 6b).

As shown above, the direction of far field stress (1st order stress) in the western part of the Eastern Alps changed in a simple way: 1) NW-directed compression in the Late Cretaceous, 2) NNE-directed compression in the Paleocene/Eocene and 3) NNW-directed compression in the Oligocene/Miocene (Fig. 25). The complex deformational history as shown by the analysis of fault planes above is the result of creation of local stress fields by strain partitioning and faulting during orogen-parallel extension (2nd order stress). These stress fields can be expected to follow each other systematically. On outcrop scale, the formation of structures related to 2nd order stress is accompanied by local stress fields (3rd order stress). Mechanisms creating 3rd order stress include shearing within shear zones with large offset, spreading of material parallel to fold axes during folding or extension above a neutral surface during flexural folding. These stress fields will not show any systematic succession of events.

5 Acknowledgements

The author was supported by the Austrian Science foundation (Project P13566-TEC). The ideas presented in this papers were developed and modified by discussions with F. Reiter, R. Brandner, K. Decker, C. Tomek and O. A. Pfiffner. Many thanks to A. Gruber and F. Reiter for assistence in the field and to Ch. Prager, who supplied unpublished fault data.

References

Angelier, J. & Goguel, J. (1979): Sur une méthode simple de détermination des axes principaux des contraintes pour une population de failles.- C. R. Acad. Sci. Paris, 288, 307 - 310, Paris.

Auer, M. & Eisbacher, G. H. (2003): Deep structure and kinematics of the Northern Calcareous Alps (TRANS-ALP profile).- Int. J. Earth Sci., 92, 210-227, 20 Abb., Stuttgart.

Bachmann, G. H., Dohr, G. & Müller, M. (1982): Exploration in a classic thrust belt and its foreland: Bavarian Alps, Germany.- AAPG Bull., 66, 2529-2542, 11 Abb., Tulsa.

Böhm, F., Dommergues, J. - L. & Meister, C. (1995): Breccias of the Adnet Formation: indicators of a Mid-Liassic tectonic event in the Northern Calcareous Alps (Salzburg/Austria).- Geol. Rundsch., 84, 272-286, 12 Abb., Stuttgart.

Brix, F. & Schultz, O. (1993): Erdöl und Erdgas in Österreich.- Veröff. Nat.-hist. Mus. Wien, 19 (2. Auflage), 668 p., 200 Abb., 62 Tab., 17 Taf., Horn (Berger).

Brügel, A. (1998): Provenances of alluvial conglomerates from the Eastalpine foreland: Oligo-/Miocene denudation history and drainage evolution of the Eastern Alps.- Tübinger geowiss. Arb., 40, 168 p., 65 Abb., 10 Tab., Tübingen.

Castellarin, A. & Cantelli, L. (2000): Neo-Alpine evolution of the Southern Eastern Alps.- Journal of Geodynamics, 30, 251-274, 10 Abb., Oxford.

Channell, J. E. T., Brandner, R., Spieler, A. & Smathers, N. P. (1990): Mesozoic paleogeography of the Northern Calcareous Alps - evidence from paleomagnetism and facies analysis.- Geology, 18, 828 - 831, 5 Abb., Boulder.

Channell, J. E. T, Brandner, R., Spieler, A. & Stoner, J. S. (1992): Paleomagnetism and paleogeography of the Northern Calcareous Alps (Austria).- Tectonics, 11, 792 - 810, 20 Abb., 3 Tab., Washington.

Dallmeyer, R. D., Handler, R., Neubauer, F. & Fritz, H. (1998): Sequence of thrusting within a thick-skinned tectonic wedge: Evidence from 40Ar/39Ar and Rb/Sr ages from the Austroalpine nappe complex of the Eastern Alps.- Journal of Geology, 106, 71-86, Chicago.

Decker, K., Meschede, M. & Ring, U. (1993): Fault Slip Analysis along the Northern Margin of the Eastern Alps (Molasse, Helvetic Nappes, North- and South - Penninic Flysch, and the Northern Calcareous Alps.- Tectonophysics, 223, 291 - 312, 13 Abb., 1 Tab., Amsterdam.

Decker, K., Peresson, H. & Faupl, P. (1994): Die miozäne Tektonik der östlichen Kalkalpen: Kinematik, Paläospannungen und Deformationsaufteilung während der "lateralen Extrusion" der Zentralalpen.- Jb. Geol. B.-A., 137, 5-18, 10 Abb., Wien.

Egger, H. (1992): Zur Geodynamik und und Paläogeographie des Rhenodanubischen Flysches (Neokom - Eozän) der Ostalpen.- Zeitschr. Dt. Geol. Ges., 143, 51 - 65, 7 Abb., Hannover.

Eisbacher, G. & Brandner, R. (1995): Role of high-angle faults during heteroaxial contraction, Inntal thrust sheet, Northern Calcareous Alps, western Austria.- Geol.-Paläontol. Mitt. Univ. Innsbruck, 20, 389 - 406, 7 Abb., Innsbruck.

Eisbacher, G. H. & Brandner, R. (1996): Superposed fold thrust structures and high angle faults, northwestern Calcareous Alps, Austria.- Ecl. Geol. Helv., 89, 553 - 571, 4 Abb., 2 Taf., Basel.

Ferreiro - Mählmann, R. (1994): Zur Bestimmung von Diagenesehöhe und beginnender Metamorphose -Temperaturgeschichte und Tektogenese des Austroalpins und Südpenninikums in Vorarlberg und Mittelbünden.- Frankfurter geowiss. Abh., Serie C, Mineralogie, 14, 498 p., Frankfurt.

Frisch, W., Dunkl, I. & Kuhlemann, J. (2000): Post-collisional orogen-parallel large-scale extension in the Eastern Alps.- Tectonophysics, 327, 239-265, Amsterdam.

Frisch, W., Kuhlemann, J., Dunkl, I. & Brügel, A. (1998): Palinspastic reconstruction and topographic evolution of the Eastern Alps during late Tertiary tectonic extrusion.- Tectonophysics, 297, 1 - 15, 4 Abb., Amsterdam.

Froitzheim, N., Conti, P. & Van Daalen, M. (1997): Late Cretaceous, synorogenic, low-angle normal faulting along the Schlinig fault (Switzerland, Austria) and its significance for the tectonics of the Eastern Alps.- Tectonophysics, 280, 267 - 293, 13 Abb., Amsterdam.

Froitzheim, N. & Manatschal, G. (1996): Kinematics of Jurassic rifting, mantle exhumation, and passive-margin formation in the Austroalpine and Penninic nappes (eastern Switzerland).- Geol. Soc. Am. Bull., 108, 1120 - 1133, 10 Abb., Boulder.

Froitzheim, N., Schmid, S. M. & Frey, M. (1996): Mesozoic paleogeography and the timing of eclogite-facies metamorphism in the Alps: A working hypothesis.- Ecl. Geol. Helv., 89, 81-110, 5 Abb., 1 Taf., Basel.

Froitzheim, N., Schmid, St. & Conti, P. (1994): Repeated change from crustal shortening to orogen parallel extension in the Austroalpine units of Graubünden.- Ecl. Geol. Helv., 87, 559 - 612, 15 Abb., 1 Tab., Basel.

Fuchs, W. (1976): Gedanken zur Tektogenese der nördlichen Molasse zwischen Rhone und March.- Jb. Geol. B.-A., 119, 207 - 249, 1 Tab., 2 Taf., Wien.

Fuchs, W. (1980): Die Molasse des Unterinntales.- In: Oberhauser, R. (Ed.): Der geologische Aufbau Österreichs, 152 - 155, 1 Abb., Wien (Springer).

Fügenschuh, B., Mancktelow, N. S. & Seward, D. (2000): Cretaceous to Neogene cooling and exhumation history of the Ötztal-Stubai basement complex, eastern Alps: A structural and fission track study.- Tectonics, 19, 905-918, 7 Abb., Washington, D.C..

Fügenschuh, B., Seward, D. & Mancktelow, N. (1997): Exhumation in a convergent orogen: the western Tauern window.- Terra Nova, 9, 213 - 217, 3 Abb., Oxford.

Gawlick, H. - J., Frisch, W., Vecsei, A., Steiger, T. & Böhm, F. (1999): The change from rifting to thrusting in the Northern Calcareous Alps as recorded in Jurassic sediments.- Geol. Rundsch., 87, 644 - 657, 10 Abb., Stuttgart.

Gruber, A. (1995): Öffnung und Schließung von tertiären Becken im Bereich des Eiberger Beckens Unterinntal, Tirol) - Ein Beitrag zur Unterinntal- Scherzone.- Unpubl. Dipl. Arb. Univ. Innnsbruck, 150 S., Innsbruck

Gruber, A. (1997): Stratigraphische und strukturelle Analyse im Raum Eiberg (Nördliche Kalkalpen, Unterinntal, Tirol) unter besonderer Brücksichtigung der Entwicklung in der Oberkreide und Tertiär.- Geol.-Paläontol. Mitt. Univ. Innsbruck, 22, 159 - 197, 17 Abb., 10 Taf., Innsbruck.

Grundmann, G. & Morteani, G. (1985): The Young Uplift and the Thermal History of the Central Eastern Alps (Austria/Italy), Evidence from Apatite Fission Track Ages.- Jb. Geol. Bundesanst., 128, 197 - 216, 13 Abb., 2 Tab., Wien.

Hagn, H. (1981): Helvetikum.- In: Hagn, H. (Eds.): Die bayerischen Kalkalpen und ihr Vorland aus mikropaläontologischer Sicht, Geol. Bav., 82, 41 - 46, München.

Hancock, P. L. (1985): Brittle microtectonics: principles and practice.- Jour. Struct Geol., 7, 437 - 457, 19 Abb., Oxford.

Hebbeln, D., Henrich, R., Lackschewitz, S. & Ruhland, G. (1996): Tektonische Struktur und fazielle Gliederung der Lechtaldecke am NW-Rand des Tirolischen Bogens in den Chiemgauer Alpen.- Mitt. Ges. Geol. Bergbaustud. Österr., 39/40, 221-235, Wien.

Hufnagel, H., Kuckelkorn, K., Wehner, H. & Hildebrand, G. (1981): Interpretation des Bohrprofils Vorderriß auf-

grund organo-geochemischer und geophysikalischer Untersuchungen.- Geol. Bav., 81, 123-143, 6 Abb., 3 Tab., München.

Kleinspehn, K. L., Pershing, J. & Teyssier, Ch. (1989): Paleostress Stratigraphy: A new technique for analyzing tectonic control on sedimentary basin subsidence.- Geology, 17, 253 - 256, Boulder.

Kralik, M., Krumm, H. & Schramm, J. M (1987): Low Grade and Very Low Grade Metamorphism in the Northern Calcareous Alps and in the Greywacke Zone: Illite - Cristallinity Data and Isotopic Ages.- In: Faupl, P. & Flügel, H. W. (Eds.): Geodynamics of the Eastern Alps, 164 - 178, Wien (Deuticke).

Krumm, H. (1984): Anchimetamorphose im Anis und Ladin (Trias) der nördlichen Kalkalpen zwischen Arlberg und Kaisergebirge. Ihre Verbreitung und deren baugeschichtliche Bedeutung.- Geol. Rundsch., 73, 223 - 257, 13 Abb., Stuttgart.

Lackschewitz, K. S., Grützmacher, U. & Henrich, R. (1991): Paleooceanography and rotational block faulting in Jurassic carbonate series of the Chiemgau Alps (Bavaria).- Facies, 24, 1-24, Erlangen.

Lammerer, B. & Weger, M. (1998): Footwall uplift in an orogenic wedge: the Tauern Window in the Eastern Alps of Europe.- Tectonophysics, 285, 213 - 230, 13 Abb., Amsterdam.

Laubscher, H. P. (1983): Detachment, shear and compression in the Central Alps.- Geol. Soc. Am. Mem., 158, 191-211, Boulder.

Mandl, G. (1988): Mechanics of tectonic faulting: models and basic concepts.- Developments in Structural Geology 1, 407 p., Amsterdam (Elsevier).

May, T. & Eisbacher, G. (1999): Tectonics of the synorogenic "Kreideschiefer basin", northwestern Calcareous Alps, Austria.- Ecl. Geol. Helv., 92, 307-320, 15 Abb., Basel.

Müller - Wolfskeil, P. & Zacher, W. (1984): Neue Ergenisse zur Tektonik der Allgäuer und Vilser Alpen.- Geol. Rundsch., 73, 321-335, 9 Abb., Stuttgart.

Neubauer, F. (1987): The Gurktal thrust system with in the Austroalpine region - some structural and geometrical aspect.- In: Faupl, P. & Flügel, H. W (Eds.): Geodynamics of the Eastern Alps, 226-236, 4 Abb., Wien (Deuticke).

Neubauer, F., Dallmeyer, R. D., Dunkl, I. & Schirnik, D. (1995): Late Cretaceous exhumation of the metamorphic Gleinalm dome, Eastern Alps: kinematics, cooling history and sedimentary response in a sinistral wrench corridor.- Tectonophysics, 242, 79 - 98, 13 Abb., 2 Tab., Amsterdam.

Neubauer, F., Genser, J. & Handler, R. (2000): The Eastern Alps: Result of a two stage collision process.- Mitt. Österr. Geol. Ges., 92, 117-134, 8 Abb., Wien.

Niederbacher, P. (1982): Geologisch - tektonische Untersuchungen in den südöstlichen Lechtaler Alpen (Nördliche Kalkalpen, Tirol).- Geol.-Paläontol. Mitt. Univ. Innsbruck, 12, 123 - 154, 15 Abb., 2 Tab., Innsbruck.

Nievergelt, P., Liniger, M., Froitzheim, N. & Ferrero-mählmann, R. (1996): Early to mid Tertiary crustal extension in the Central Alps: The Turba Mylonite Zone (Eastern Switzerland).- Tectonics, 15/2, 329 - 340, 6 Abb., Washington, D.C.

Ortner, H. (1996): Deformation und Diagenese im Unterinntaler Tertiär (zwischen Rattenberg und Durchholzen) und seinem Rahmen.- Unpubl. PhD. Thesis, Univ. Innsbruck, 234 S., Innsbruck.

Ortner, H. (2001): Growing folds and sedimentation of the Gosau Group, Muttekopf, Northern Calcareous Alps, Austria.- Int. Jour. Earth Sci., 90, 727-739, 9 Abb., Stuttgart.

Ortner, H., Brandner, R. & Gruber, A. (1999): Kinematic evolution of the Inn valley shear zone from Oligocene to Miocene.- In: Szekely, B., Frisch, W., Kuhlemann, J. & Dunkl, I. (Eds.): 4th Workshop on Alpine geological studies, 21 - 24. September 1999, Tübinger geowissenschaftliche Arbeiten 52, 192 - 193, Tübingen.

Ortner, H., Reiter, F. & Acs, P. (2002): Easy handling of tectonic data: the programs TectonicVB for Mac and TectonicsFP for Windows(TM).- Computers & Geosciences, 28, 1193-1200, 4 Abb., 3 Tab., Oxford.

Ortner, H., Reiter, F. & Brandner, R. (2003): Kinematics of the Inntal shear zone and its relation to other major faults crossing the northern TRANSALP sesmic section.- In: Nicolich, R., Polizzi, D. & Furlani, S. (Eds.): TRANSALP conference, extended abstracts, Mem. Sci. Geol., 54, 189-192, Padova.

Ortner, H. & Stingl, V. (2001): Facies and Basin Development of the Oligocene in the Lower Inn Valley, Tyrol/ Bavaria.- In: Piller, W. & Rasser, M. (Eds.): Paleogene in Austria, Schriftenreihe der Erdwissenschaftlichen Kommissionen, 14, 153-196, 24 Abb., Wien (Österreichische Akademie der Wissenschaften).

Ortner, H. (2003): Cementation and Tectonics in the Inneralpine Molasse of the Lower Inn Valley.- Geologisch-Paläontologische Mitteilungen der Universität Innsbruck, 26, 71-89, Innsbruck.

Ortner, H. & Stingl, V. (2003): Field Trip E1: Lower Inn Valley (Southern margin of Northern Calcareous Alps, TRANSALP Traverse).- Geol.-Paläontol. Mitt. Univ. Innsbruck, 26, 1-20, Innsbruck.

Pavoni, N. (1977): Erdbeben im Gebiet der Schweiz.- Ecl. Geol. Helv., 70, 351 - 370, 6 Abb., 1 Tab., 1 Taf., Basel.

Peresson, H. & Decker, K. (1997a): Far-field effects of late

Miocene subduction in the Eastern Carpathians: E-W Compression and inversion of structures in the Alpine Carpathian Pannonian region.- Tectonics, 16, 38 - 56, 12 Abb., 3 Tab., Washington.

Peresson, H. & Decker, K. (1997b): The Tertiary dynamics of the northern Eastern Alps (Austria): changing palaeostresses in a collisional plate boundary.- Tectonophysics, 272, 125 - 157, Amsterdam.

Petit, J.- P. & Laville, E. (1987): Morphology and Microstructures of Hydroplastic Slickensides in Sandstone.- In: Jones, M. E. & Preston, R. M. F. (Eds.): Deformation of Sediments and Sedimentary Rocks, Geol. Soc. Spec. Publ. No. 29, 107 - 121, 18 Abb., 1 Tab., London.

Petschik, R. (1989): Zur Wärmegeschichte im Kalkalpin Bayerns und Nordtirols (Inkohlung und Illit - Kristallinität).- Frankfurter geowiss. Arb., Serie C, Mineralogie, 10, 259 S., 75 Abb., 3 Taf., Frankfurt.

Pfiffner, O. A. & Hitz, L. (1996): Geologic interpretation of the seismic profiles of the Eastern Traverse (lines E1-E3, E7-E9): eastern Swiss Alps.- In: Pfiffner, O. A., Lehner, P., Heitzmann, P., Mueller, S. & Steck, A. (Eds.): Results of NRP 20: Results of NRP 20, 73-100, Basel (Birkhäuser).

Price, N. J. & Cosgrove, J. W. (1991): Analysis of Geological Structures.- 502 p., Cambridge (Cambridge University Press).

Ratschbacher, L., Frisch, W., Linzer, G. & Merle, O. (1991): Lateral extrusion in the Eastern Alps, Part 2: Structural analysis.- Tectonics, 10, 257 - 271, 8 Abb., 1 Tab., Washington.

Ratschbacher, L. & Neubauer, F. (1989): West-directed décollement of Austro-Alpine cover nappes in the Eastern Alps: geometrical and rheological considerations.- In: Coward, M. P., Dietrich, D. & Park, R. G. (Eds.): Alpine Tectonics, Geological Society of London Special Publication No. 45, 243 - 262, 12 Abb., 1 Tab., London.

Reiter, F. (2000): Strukturell - stratigraphische Neubearbeitung der „Schwazer Trias" westlich des Zillertales.- Unpubl. Dipl. Thesis, Univ. Innsbruck, 179 p., Innsbruck.

Sausgruber, T. (1994): Jurabeckenentwicklung nördlich vom Achensee und deren Folgen bei der alpidischen Kompressionstektonik.- Unpubl. Dipl. Thesis, Univ. Innsbruck, 133 p., Innsbruck

Schmid, S. M. & Froitzheim, N. (1993): Oblique Slip and Block Rotation along the Engadine Line.- Eclogae Geol. Helv., 86, 569 - 593, 6 Abb., 1 Taf., Basel.

Schmid, S. M. & Haas, R. (1989): Transition from Near Surface Thrusting to Intrabasement Decollement: Schlinig Thrust, Eastern Alps.- Tectonics, 8, 697 - 718, 14 Abb., Washington.

Schmid, S., Pfiffner, O. A. & Schreurs, G. (1997): Rifting and collision within the Penninic zone of eastern Switzerland.- In: Pfiffner, O. A., Lehner, P., Heitzmann, P., Mueller, S. & Steck, A. (Eds.): Deep structure of the Swiss Alps: Results of NRP 20, 160-185, Basel (Birkhäuser).

Schrader, F. (1988): Das regionale Gefüge der Drucklösungsdeformation an Geröllen im westlichen Molassebecken.- Geol. Rundsch., 77, 347 - 369, 6 Abb., Stuttgart.

Sleijko, D., Carulli, G. B., Carraro, F., Castaldini, D., Cavallin, A., Doglioni, C., Iliceto, V., Nicolich, R., Rebez, A., Semenza, E., Zanferrari, A. & Zanolla, Z. (1987): Modello Sismotettonico dell`Italia Nord-Orientale.- Consiglio Nazionale Delle Ricerce, Gruppo Nazionale per la Difesa dai Terremoti, Rendiconto n. 1, 82 S., 27 Abb., 2 Tab., 3 Taf., Trieste.

Sperner, B., Ratschbacher, L. & Ott, R. (1993): Fault Striae Analysis: A Turbo - Pascal Program Package for Graphical Presentation and Reduced Stress Tensor Calculation.- Computers & Geosciences, 19, 1361 - 1388, 4 Abb., 3 Tab., Oxford.

Stampfli, G. M., Mosar, J., Marquer, R., Marchant, R., Baudin, T. & Borel, G. (1998): Subduction and obduction processes in the Swiss Alps.- Tectonophysics, 296, 159 - 204, 18 Abb., Amsterdam.

Thiele, O. (1976): Der Nordrand des Tauernfensters zwischen Mayrhofen und Innerschmirn (Tirol).- Geol. Rundsch., 65, 410-421, Stuttgart.

Thöni, M. (1981): Degree and Evolution of the Alpine Metamorphism in the Austroalpine Unit W of the Hohe Tauern in the Light of K/Ar and Rb/Sr Age Determination on Micas.- Jb. Geol. Bundesanst., 124, 111 - 174, 12 Abb., 16 Tab., Wien.

Tollmann, A. (1985): Geologie von Österreich, Band 2.- 710 p., 286 Abb., 27 Tab., Wien (Deuticke).

Transalp Working Group (2002): First deep seismic reflection images of the Eastern Alpsreveal giant crustal wedges and transcrustal ramps.- Geophysical Reasearch Letters, 29, 92-1 - 92-4, Washington, D.C..

Wächter, J. (1987): Jurassische Massflow- und Internbrekzien und ihr sedimentär-tektonisches Umfeld im mittleren Abschnitt der nördlichen Kalkalpen.- Bochumer geol. und geotechn. Arbeiten, 27, 239 p., 51 Abb., 12 Taf., Bochum.

Wagreich, M. & Decker, K. (2001): Sedimentary tectonics and subsidence modelling of the type Upper Cretaceous Gosau basin (Northern Calcareous Alps, Austria).- Int. Jour. Earth Sci., 90, 714-726, 10 Abb., 3 Tab., Stuttgart.

Weh, M. & Froitzheim, N. (2001): Penninic cover nappes in the Prättigau half-window (Eastern Switzerland):

Structure and Tectonic evolution.- Ecl. Geol. Helv., 94, 237-252, Basel.

Woijtal, S. & Pershing, J. (1991): Paleostresses associated with faults of large offset.- Journal of Structural Geology, 13, 49 - 62, 8 Abb., Oxford.

Zerbes, D. & Ott, E. (2000): Geologie des Kaisergebirges (Tirol): Kurzerläuterung zur geologischen Karte 1:25.000 und Exkursionsvorschläge.- Jb. Geol. B.-A., 142, 95-143, 34 Abb., 1 Taf., Wien.

Zweigel, J., Aigner, T. & Luterbacher, H. (1998): Eustatic versus tectonic controls an Alpine foreland basin fill: sequence stratigraphy and subsidence analysis in the SE German Molasse.- In: Mascle, A. (Eds.): Cenozoic foreland basins of western Europe, Spec. Publ. Geol. Soc. London No. 134, 299-323, London.

Author´s address: Dr. Hugo Ortner, Institut für Geologie und Paläontologie, Universität Innsbruck, Innrain 52, 6020 Innsbruck
email: hugo.ortner@uibk.ac.at